



Understanding the uncertainty in global forest carbon turnover

Thomas A. M. Pugh¹, Tim T. Rademacher^{2,3,4}, Sarah L. Shafer⁵, Jörg Steinkamp^{6,7}, Jonathan Barichivich^{8,9}, Brian Beckage¹⁰, Vanessa Haverd¹¹, Anna Harper¹², Jens Heinke¹³, Kazuya Nishina¹⁴, Anja Rammig¹⁵, Hisashi Sato¹⁶, Almut Arneth¹⁷, Stijn Hantson¹⁸, Thomas Hickler^{6,19}, Markus Kautz²⁰, Benjamin Quesada^{17,21}, Benjamin Smith^{22,23}, Kirsten Thonicke¹³

¹ School of Geography, Earth & Environmental Sciences and Birmingham Institute of Forest Research, University of Birmingham, Birmingham, B15 2TT, United Kingdom.

² Department of Organismic and Evolutionary Biology, Harvard University, Cambridge, MA 02138, USA.

³ School of Informatics, Computing and Cyber Systems, Northern Arizona University, Flagstaff, AZ 86011, USA.

10 ⁴ Center for Ecosystem Science and Society, Northern Arizona University, Flagstaff, AZ 86011, USA.

⁵ Geosciences and Environmental Change Science Center, U.S. Geological Survey, 3200 SW Jefferson Way, Corvallis, OR 97331, USA.

⁶ Senckenberg Biodiversity and Climate Research Centre (BiK-F), Senckenberganlage 25, 60325 Frankfurt/Main, Germany.

⁷ Johannes Gutenberg-University Mainz, Anselm-Franz-von-Bentzel-Weg 12, 55128 Mainz, Germany.

15 ⁸ Instituto de Conservación Biodiversidad y Territorio, Universidad Austral de Chile, Valdivia, Chile.

⁹ Laboratoire des Sciences du Climat et de l'Environnement, IPSL, CNRS/CEA/UVSQ, 91191 Gif sur Yvette, France.

¹⁰ Department of Plant Biology & Department of Computer Science, University of Vermont, Burlington, VT 05405, USA.

¹¹ CSIRO Oceans and Atmosphere, PO Box 3023, Canberra, ACT 2601, Australia.

¹² College of Engineering, Mathematics, and Physical Sciences, University of Exeter, Exeter, UK

20 ¹³ Potsdam-Institute for Climate Impact Research (PIK), Telegraphenberg, 14473 Potsdam, Germany.

¹⁴ Center for Regional Environmental Studies, National Institute for Environmental Studies (NIES), 16-2, Onogawa, Tsukuba, Japan

¹⁵ Technical University of Munich (TUM), School of Life Sciences Weihenstephan, Freising, Germany.

25 ¹⁶ Institute of Arctic Climate and Environment Research (IACE), Japan Agency for Marine-Earth Science and Technology (JAMSTEC), 3173-25 Showamachi, Kanazawa-ku, Yokohama, 236-0001, Japan.

¹⁷ Karlsruhe Institute of Technology, Institute of Atmospheric Environmental Research (IMK-IFU), Kreuzeckbahnstrasse 19, 82467, Garmisch-Partenkirchen, Germany.

¹⁸ Department of Earth System Science, University of California, Irvine, CA, USA.

¹⁹ Department of Physical Geography, Goethe University, Altenhöferallee 1, 60348 Frankfurt/Main, Germany.

30 ²⁰ Department of Forest Protection, Forest Research Institute Baden-Württemberg, 79100 Freiburg, Germany.

²¹ Universidad del Rosario, Faculty of Natural Sciences and Mathematics, Research Group "Interactions Climate-Ecosystems (ICE)", Cra 26 63b-48, 111221, Bogotá, Colombia

²² Department of Physical Geography and Ecosystem Science, Lund University, 22362 Lund, Sweden.

²³ Hawkesbury Institute for the Environment, Western Sydney University, Locked Bag 1797, Penrith NSW 2751, Australia.

35 Correspondence to: Thomas A. M. Pugh (t.a.m.pugh@bham.ac.uk)

Abstract. The length of time that carbon remains in forest biomass is one of the largest uncertainties in the global carbon cycle, with both recent-historical baselines and future responses to environmental change poorly constrained by available observations. In the absence of large-scale observations, models tend to fall back on simplified assumptions of the turnover rates of biomass and soil carbon pools to make global assessments. In this study, the biomass carbon turnover times calculated by an ensemble of contemporary terrestrial biosphere models (TBMs) are analysed to assess their current capability to accurately estimate biomass carbon turnover times in forests and how these times are anticipated to change in the future.



45 Modelled baseline 1985-2014 global forest biomass turnover times vary from 12.2 to 23.5 years between models. TBM
differences in phenological processes, which control allocation to and turnover rate of leaves and fine roots, are as important
as tree mortality with regard to explaining the variation in total turnover among TBMs. The different governing mechanisms
50 exhibited by each TBM result in a wide range of plausible turnover time projections for the end of the century. Based on these
simulations, it is not possible to draw robust conclusions regarding likely future changes in turnover time for different regions.
Both spatial and temporal uncertainty in turnover time are strongly linked to model assumptions concerning plant functional
type distributions and their controls. Twelve model-based hypotheses are identified, along with recommendations for
pragmatic steps to test them using existing and novel observations, which would help to reduce both spatial and temporal
uncertainty in turnover time. Efforts to resolve uncertainty in turnover time will need to address both mortality and
establishment components of forest demography, as well as key drivers of demography such as allocation of carbon to woody
versus non-woody biomass growth.

1 Introduction

55 Large uncertainties persist in the magnitude and direction of the response of the terrestrial carbon cycle to changes in climate,
atmospheric CO₂ concentration, and nutrient availability (Ciais et al., 2013; Friedlingstein et al., 2014), which prevent
definitive statements on carbon-cycle climate feedbacks (Arneth et al., 2010; Ciais et al., 2013). Carbon uptake and turnover
by forests is a very large component in the global carbon cycle on the scale of decades to centuries (Carvalhais et al., 2014;
Jones et al., 2013). The gain or loss of carbon in terrestrial ecosystems is a function of net carbon input to the system, via net
primary productivity (NPP), and the rate of carbon turnover (loss) in the system. For vegetation this can be formalised as:

60

$$dC_{veg}/dt = NPP - F_{turn} = NPP - C_{veg}/\tau \quad (\text{Eq. 1}),$$

where F_{turn} is the total loss flux of live biomass due to the transfer of plant tissue to dead pools of litter and soil, to harvest
products and residues, or to the atmosphere via burning. C_{veg} is the stock of carbon in live biomass and τ the mean residence
65 (turnover) time of that live biomass. Neither NPP nor τ are constant but are affected by many factors including climate,
physiological stress, disturbances, species, functional group or ecosystem type. Some, but not all, relevant dependencies of τ
on its drivers are represented in current vegetation models. Until recently, most attention has instead focussed on understanding
spatial and temporal dynamics of NPP and respiration carbon losses (e.g. Ahlström et al., 2015a, 2012; Ballantyne et al., 2017;
Cramer et al., 1999; Schaphoff et al., 2006). More recently, an increasing number of studies have found τ to have comparable
70 or even larger importance than NPP when assessing the response of C_{veg} to environmental change using terrestrial biosphere
models (TBMs) (Ahlström et al., 2015a; Friend et al., 2014; Galbraith et al., 2013; Johnson et al., 2016; Parazoo et al., 2018;
Thurner et al., 2017), with large divergence in TBM projections of τ over the 21st century. This divergence is primarily due to
TBM structure and parameterisation (Nishina et al., 2015), but the reasons underlying it have not been closely analysed.



75 Conceptually, turnover time of carbon in live vegetation is a function of carbon allocation to biomass pools with different
characteristic turnover times, and changes in these characteristic turnover times in response to environmental variation.
Moreover, TBMs typically aim to represent the landscape across hundreds or thousands of square kilometres. At this scale,
not only individual plant behaviour, but also changes in the functional species composition, affect τ . Under environmental
change, there are several mechanisms by which τ and biomass may be altered (Table 1). Thus, effects of environmental change
80 on τ can be divided into three groupings, those associated with changes to allocation patterns of individual trees within the
current mix of species (denoted MI in Table 1), those associated with collective responses of multiple individuals at the stand
level (MS) and those associated with a population-level change in species mix (MP).

Most carbon in forest vegetation is stored in wood as a result of its relatively long turnover times compared to soft tissues such
85 as leaves, fine roots and fruits. Turnover of wood is believed to primarily result from tree mortality, although branchfall is also
poorly quantified (Marvin and Asner, 2016). Harvest aside, mortality in trees can have many causes, including both primarily
biotic (e.g. competition, insects, senescence) and abiotic (e.g. fire, drought, windthrow) causes, often with complex interactions
between mechanisms and forest structure (Brando et al., 2014; Franklin et al., 1987). Compared to the study of productivity,
quantitative understanding of tree mortality is at a fledgling stage, with large unknowns relating to the actual process of death
90 and their environmental dependencies (Anderegg et al., 2016; Hartmann et al., 2018; McDowell et al., 2008; Sevanto et al.,
2014). Accordingly, neither plant-physiological processes nor interactions of multiple stresses are represented in great detail
in current TBMs, although some aspects of the hydraulic and carbohydrate system, and coupled carbon- and water-related
physiology, may be linked to mortality in these models. As reviewed in McDowell et al. (2011) and Adams et al. (2013) (see
also Section 2.2 herein), TBMs often prescribe bioclimatic limits for establishment and survival, or threshold temperatures
95 combined with how often the threshold is exceeded to determine mortality. Vitality-based processes, such as maintenance of
a positive carbon balance or a minimum threshold of growth efficiency (ratio of productivity to leaf area), may also result in
tree mortality. In some TBMs, vitality-based processes are supplemented or replaced by self-thinning rules (e.g. Haverd et al.,
2014; Sitch et al., 2003). Mortality in association with disturbance, such as storms or insect outbreaks, are captured in some
TBMs by a set “background” mortality, the likelihood of which may be size or age related (e.g. Smith et al., 2014). Fires are
100 now represented in many TBMs, however the representation of the impact of fire on the vegetation is still immature (Hantson
et al., 2016). Ultimately, the effect of a change in mortality rate on τ may be either direct (Table 1, MI_{MR}), or indirect, via shifts
in tree functional composition (possibly mediated by MI_{MR}) that change the mean behaviour of the tree population at the
landscape scale (MP).

105 As for wood, turnover rates of soft tissues due to phenological cycles also lack strong constraints, with fine root turnover being
challenging to measure (Lukac, 2012), reproductive investment differing widely between species and life stage (Wenk and



110 Falster, 2015) and very little data on root exudation rates available for any ecosystem (Pugh et al., 2016). Even leaf turnover
rate suffers from uncertainty over leaf longevity, particularly in evergreen trees, and herbivory rates. Although the carbon stock
in soft tissues may be relatively small compared to wood, these phenological turnover rates influence the amount of carbon
115 that trees must allocate to maintain a given leaf area or root network. Uncertainties in phenological turnover rates will influence
overall biomass τ in TBMs, as they affect the amount of carbon available for allocation to wood. Allocation patterns within a
given plant or plant type may also change as a function of environmental conditions (MI_{RA}), for instance based on a "functional
balance" principle in which resources are allocated to try to alleviate the most limiting constraint(s) (Franklin et al., 2012;
Sitch et al., 2003). Studies that include how vegetation composition evolves with climate often include effective allocation
120 shifts at the population level in calculations of τ (MP_{RA}). Overall, changes in phenological turnover rates, either at the individual
level (MI_{ST}), or through vegetation composition shifts (MP_{ST}) may have profound influences on τ .

Changes in productivity affect biomass accumulation ($MI_{NPP,F}$, MP_{NPP}) but do not affect τ directly. However, they may
accelerate the self-thinning process (MS_{comp}) and also change mortality rate through the link to tree vitality (Bugmann and
120 Bigler, 2011). Furthermore, if changes in productivity are accompanied by an allocation response by the plant, for instance a
reduced allocation to leaves and stems in favour of roots as soil resources become limiting ($MI_{NPP,FS}$), then τ will be impacted.

Here, an ensemble of six representative current TBMs (Table 2) was analysed to compare assumed mechanisms governing
vegetation carbon turnover and their impacts on modelled carbon pools and fluxes (Table 3). Building on previous work (e.g.
125 Friend et al., 2014), the aims were to:

- 1) assess the baseline variation in τ within and between TBMs and identify the reasons for these variations;
- 2) evaluate the simulated τ and its components against existing observations where available;
- 3) diagnose why projections of future τ diverge between models;
- 4) identify model-based hypotheses for the spatial and temporal variation in τ to guide future research to better constrain
130 terrestrial carbon cycling.

Our analysis is restricted to forests, which contain the vast majority of vegetation carbon (Carvalhais et al., 2014). Land-use
change and management has profoundly changed biomass turnover rates over the last centuries (Erb et al., 2016), but is
disregarded here in order to focus attention on the intrinsic dynamics of forests. Dynamic changes in vegetation composition
driven by dispersal and migration are included, but only within the area currently defined as forest.



135 2. Methods

2.1 Definition of τ

Following Eq. 1, $\tau = C_{veg}/F_{turn}$ (henceforth τ_{turn}) (Sierra et al., 2017). However, τ is often approximated by C_{veg}/NPP (henceforth τ_{NPP}) (Erb et al., 2016; Thurner et al., 2017), based on the assumption that the system is in pseudo-equilibrium, and therefore $F_{turn} = NPP$ in the multiannual mean. Even in a system under transient forcing, at the global level τ_{NPP} is likely a close
140 approximation of τ_{turn} (see results in Table 4). Generally, τ_{turn} is used herein because it directly represents turnover, apart from in Fig. 1, where τ_{NPP} is used to maintain maximum consistency with the satellite-based data. In the text, where the difference between τ_{NPP} and τ_{turn} is of minimal consequence, τ is used for simplicity. Turnover time due to mortality, τ_{mort} is defined as C_{veg}/F_{mort} , where F_{mort} is the total mortality flux due to tree mortality events, i.e., leaf, root and reproductive turnover are excluded.

145 2.2 Model descriptions

The TBMs in this study (Table 2) have been widely applied in studies of the regional and global terrestrial biosphere and in major international assessments (Jones et al., 2013; Le Quéré et al., 2018; Sitch et al., 2008). They simulate the fluxes of carbon between the land surface and the atmosphere, and the cycling of carbon through vegetation and soils. All models simulate the stocks of, and fluxes to and from, wood, leaves and fine roots. A representative range of alternate modelling
150 approaches are encapsulated in this ensemble. Three of the models adopt average-individual approaches to vegetation representations (LPJmL3.5, ORCHIDEE, JULES), two a cohort-based approach (LPJ-GUESS, CABLE-POP), and one an individual-based approach (SEIB-DGVM). LPJ-GUESS includes a coupled carbon-nitrogen cycle, while all except CABLE-POP include dynamic changes in plant functional type (PFT) composition in response to environmental conditions. The number and type of PFTs vary between the models and are summarised in Table S1. Between them, the models capture many
155 of the mortality process representations currently used (Table 3). Parameters relating to phenological turnover rate are summarised in Table S2.

2.3 Model experiments

Two simulations were completed by each TBM: a historical 1901-2014 simulation, driven by the CRU-NCEP v5 observation-based climate product and observed atmospheric CO₂ mixing ratios (Le Quéré et al., 2015); and a historical-to-future 1901-
160 2099 simulation driven by IPSL-CM5A-LR RCP 8.5 climate data, bias-corrected against the observation-based WATCH dataset, as described in Hempel et al. (2013). Deposition of reactive nitrogen species (LPJ-GUESS only) was forced by data from Lamarque et al. (2013). Simulations were of potential natural vegetation (i.e. no anthropogenic land-use was applied), with the exception of CABLE-POP which does not have dynamic vegetation and thus landcover for the year 1700 was applied. CABLE-POP also differed from the other models in using the CRU-NCEP v7 climate product. Model-standard methods for



165 spin-up were applied, with spin-up CO₂ mixing ratio and nitrogen deposition fixed at 1901 values. All simulations were performed at 0.5° × 0.5° grid resolution, with the exception of JULES, which used an 1.875° × 1.25° grid cell size.

In addition to commonly used variables such as NPP, leaf area index (LAI) and C_{veg} for wood, leaves and fine roots, all TBMs also outputted separately the fluxes of carbon turnover from leaf and fine root turnover, and from each individual mortality
170 process within the model (with the exception of ORCHIDEE, which provided all mortality-driven turnover as a single value). For display purposes, these processes were conceptually grouped as described in Table 3. For those models that include a loss of carbon due to reproduction, it was either output directly, or calculated in postprocessing as 10% of NPP, consistent with the parameterisation in the model. Unless otherwise stated, results are presented as statistics over a 30-year period, which is 1985-2014 in the baseline case.

175 2.4 Analysis

Forest masking: A mask defining forest was developed for each TBM and used for subsequent analyses. For maps of TBM output, values were displayed if (1) the TBM simulated forest for a grid cell and (2) observations for the year 2000 showed the grid cell to contain at least 10% cover of closed-canopy forested area. For calculating regional sums and statistics of TBM output, the second step was implemented by multiplying the TBM output for a grid cell by the observed closed-canopy forested
180 area in that grid cell before calculating statistics. This process results in sums and statistics for each model being calculated over a slightly different area but avoids turnover statistics for forest being skewed where a TBM erroneously simulates grassland where satellite observations indicate forest. Forest distribution maps for simulations and observations and their discrepancies are shown in Fig. S1.

185 The masks identifying grid cells where each TBM simulated forest were based on simulated PFT maximum annual LAI values modified by PFT cover fraction for each grid cell. For each year, the classification “forest” was assigned to a grid cell if (a) the maximum annual LAI value summed for all simulated tree PFTs was > 2.5 or (b) the maximum annual LAI value summed for all simulated tree PFTs was > 0.5 and the PFT with the maximum LAI for the grid cell was a boreal tree PFT (i.e., boreal needleleaved evergreen, boreal needleleaved deciduous, or boreal broadleaved deciduous; Hickler et al., 2006; Smith et al.,
190 2014). For JULES and CABLE-POP, which did not break out PFTs into boreal and temperate categories, needleleaved evergreen, needleleaved deciduous, and broadleaved deciduous tree PFTs were considered potential boreal PFTs for step (b). In a final step, a grid cell was assigned as forest in the forest mask for each TBM if either condition (a) or (b) were satisfied for at least 10 years during the period 1985-2014.

195 So that only recent-historical forest area is considered, the second forest masking step was based on year 2000 satellite remote-sensing of forest cover (Pugh et al., 2019a). Forest cover at ca. 30 × 30 m (Hansen et al., 2013) was aggregated to 30 × 30 arc



seconds, and designated as closed-canopy forest if canopy coverage exceeded 50% of the aggregated grid cell. Percentage closed-canopy forest coverage was then calculated for each $0.5^\circ \times 0.5^\circ$ grid cell (each $1.875^\circ \times 1.25^\circ$ grid cell for JULES). Grid cells with less than 10% closed-canopy forest cover by this definition are not displayed on the maps, but data from these
200 grid cells are used in the global and regional sums and statistics for the TBMs.

Observation-based forest type classification: Forest type was defined as in Pugh et al. (2019b) based on the latest landcover product from the European Space Agency (ESA, 2017). The mapping of ESA landcover classes to the forest types is summarised in Table S3 and the resulting forest-type distribution is shown in Fig. S2.

205
Model forest type classification: To facilitate analysis of changes in forest composition, PFTs were classified into seven forest types (Table S1) based on phenological traits. LAI (1985-2014, 30-year mean) for all the PFTs within each forest type was summed, and the grid cell was assigned a forest type according to the grouping with the highest LAI sum. This process produced a forest-type mask for each model (Fig. S1). The unification of forest types across models means that each forest
210 type may be composed of 1-3 PFTs.

Satellite-based estimates of τ_{NPP} : Satellite-derived biomass and NPP products allow τ_{NPP} to be estimated as described in Section 2.1. Here, estimates were made for all grid cells with at least 10% closed-canopy forest cover. A contemporary product of total (above- and below-ground) vegetation carbon as prepared by Carvalhais et al. (2014), based on Saatchi et al. (2011)
215 and Thurner et al. (2014), was used. In order to be comparable with the TBM simulations, this observational biomass product was corrected for landcover by dividing the biomass values by closed-canopy forest area, making the assumption that biomass outside closed-canopy forests is negligible. NPP for the same period was estimated by averaging the MODIS NPP (Zhao and Running, 2010) and BETHY/DLR (Tum et al., 2016; Wißkirchen et al., 2013) products over the period 2000 to 2012 as per Thurner et al. (2017), making the assumption that NPP was uniform across the grid cell.

220
Tropical τ_{mort} evaluation: For South America, plot-level observations of above ground biomass (AGB) and turnover rate of AGB due to mortality were taken from Brienen et al. (2014, 2015). Mean values of AGB and AGB turnover rate were calculated across all census intervals at each of 274 plots. These data were summarised into a plot-mean τ_{mort} , weighting each census equally and assuming that τ_{mort} of AGB and total biomass are equivalent. For Africa and Asia/Australia, plot data were
225 taken from Galbraith et al. (2013). For each plot, the modelled value of τ_{mort} was extracted for the grid cell in which the plot was located, creating a vector of modelled τ_{mort} with the same spatial weighting as in the observations. Modelled τ_{mort} for each plot was a mean over the years between the beginning of the first census and end of the last census at that plot for the South American data, and over 1985-2014 for the other data, for which census interval information was not provided. Equivalent compilations for temperate and boreal zones were not available.



230

Drought-mortality evaluation: Very limited information on large-scale tree mortality due to extreme events is currently available for evaluating model simulations. Here, the TBMs forced by CRU-NCEP were compared to drought-related tree mortality observed at a number of sites (Allen et al., 2010, as summarised by Steinkamp and Hickler, 2015). The fraction of sites for which each TBM simulated significantly enhanced mortality in the 5 years following the observed drought-mortality event, relative to the whole simulation, was calculated with a Wilcoxon Rank Test on mortality fluxes using a 5% significance level. This fraction was compared against a likelihood of 10 randomly selected 5-year intervals seeing significantly enhanced mortality. For each TBM, only observed data from sites where the TBM simulated forest (as defined by the forest mask for each TBM) were considered.

235

3. Results

240

3.1 Recent-historical C_{veg} and τ

Simulated total C_{veg} in global closed-canopy forests ranges from 284 to 432 Pg C among models, with two distinct clusters around the extremes of this range (Table 4). Satellite-based C_{veg} over the same area is consistent with the upper end of the range at 450 Pg C, although the satellite-based estimate includes management effects not explicitly included in the model simulations here. There is large variation in the global mean of forest NPP between models (Table 4), but consistency in the relative global pattern (Fig. S3). Modelled global mean τ_{NPP} for forest vegetation varies from 11.9 to 22.6 years, comparable to the satellite-based estimate of 19.3 years. Regional variations can be even more pronounced, for instance τ_{NPP} varies from *ca.* 10 to 25 years for parts of the Amazon region, and *ca.* 5 to 30 years for parts of the boreal forest, depending on the model (Fig. 1). Particularly marked is a lack of agreement in the relative differences between regions, with four models (CABLE-POP, JULES, LPJ-GUESS, LPJmL) simulating τ_{NPP} to be longer in tropical forests than in extratropical forests, whereas ORCHIDEE and SEIB-DGVM show a much more mixed pattern (Fig. 1). The satellite-based estimate also finds τ_{NPP} to be relatively longer in the tropics than the extratropics. Notably, the global frequency distribution of τ_{NPP} from the satellite-based estimate is unimodal with a strong left-skew and a wide range of τ_{NPP} found across all forest types (Fig. 2). In contrast, τ_{NPP} distributions modelled by the TBMs are often multimodal, and in many cases characterised by distributions for individual forest types that only span a fraction of the global range in τ_{NPP} . Relative abundance of forest types also varies substantially between models (Fig. 2, Fig. S4).

245

250

255

Overall, mortality is responsible for 37 to 81% of F_{tum} , but is less than 50% of F_{tum} for four of the six models (Fig. 3). Much of this variation comes from fine roots, for which the fraction of F_{tum} varies from 6 to 37% depending on the model, whilst the fraction of F_{tum} due to leaf phenology varies from 13 to 26% (Fig. 3). These results reflect different hypotheses as to the main drivers of turnover (Table 5: H1a and H1b). Phenological and mortality turnover fluxes explain broadly comparable amounts

260



of spatial variation in the turnover flux in CABLE-POP, LPJ-GUESS, LPJmL, and ORCHIDEE (Fig. 4a) (Table 5: H2). The substantially different shapes of the density kernels for each TBM for τ_{mort} compared to τ_{NPP} (Fig. 2 vs. Fig. 5) further display the extent to which phenological processes influence F_{turn} among models.

265 Following the same logic that $F_{\text{turn}} \approx \text{NPP}$, the partitioning of F_{turn} among tissue types is approximately equal to the allocation of NPP between those tissue types. There are large disparities between the TBMs in terms of the turnover rates assigned to fine roots. For instance, JULES assumes fine root longevities 2-3 times that of the other models (Table S2), resulting in a global mean fine root carbon turnover time (τ_{fineroot}) of 5.0 years (Table 4), consistent with the very small fraction of F_{turn} realised via fine roots. In contrast, τ_{fineroot} for CABLE-POP is just 0.6 years. Leaf carbon turnover times for evergreen PFTs
270 also differ notably between TBMs (Table S2). Although the models typically reflect the empirical trade-off of leaf longevity with specific leaf area (Reich et al., 1997), the relationship is not proportional, with substantially more carbon required to maintain a canopy with leaves of one-year longevity compared to two years (Fig. S4). Large differences between the models in leaf cost for a given longevity are also apparent. Finally, the models differ in the amount of biomass required in each tissue type, for instance in the assumed ratio of leaf area to sapwood area (LA:SA). For the models herein with clearly defined LA:SA
275 (Table S4), the choice of LA:SA influences the maximum LAI simulated. For instance, LPJ-GUESS almost uniformly simulates lower LAI than LPJmL (Fig. S5), in line with the lower LA:SA used. Consistent with these differences in PFT-level parameters, spatial variation in the fraction of turnover due to phenology closely follows forest-type distribution (cf. Fig. S6 and Fig. S7) and spatial variability in phenological turnover flux was higher across than within forest types for five of the models (Fig. S8).

280 Whilst the phenological turnover flux is crucial for allocation of NPP, much larger carbon stocks are held in wood than in soft tissues. Across five of the models here, the fraction of turnover due to mortality is higher in the tropics than at higher latitudes (Fig. S6; LPJmL shows the opposite behaviour), indicating a greater relative allocation to wood compared to soft tissues in this region. However, mean turnover times due to mortality (τ_{mort}) are much less consistent between models. The tropical
285 broadleaved evergreen forest type is simulated to have the highest mean τ_{mort} by LPJmL, whilst CABLE-POP and LPJ-GUESS simulate highest mean τ_{mort} for needleleaved evergreen forest, JULES for boreal broadleaved deciduous forest and ORCHIDEE for temperate broadleaved evergreen forest (Fig. 5). Greater allocation to wood, higher τ_{mort} , or a combination of both are consistent with high tropical forest biomass, and the models reflect these alternative hypotheses (Table 5: H3). Comparison of modelled τ_{mort} with observations from tropical forest plots suggests that most of the TBMs here may substantially underestimate
290 τ_{mort} in this region (Fig. S9), suggesting that allocation of carbon to wood in the tropics might be overestimated. As for phenological turnover, spatial variation in τ_{mort} is closely linked to forest-type distribution (Fig. S8), reflecting PFT-specific mortality thresholds or likelihood functions, or even PFT-specific mortality processes (e.g. heat stress in LPJmL).



295 The wide spread in τ_{mort} across models (Table 4) and forest types (Fig. 5) reflects the range of approaches used to represent mortality. However, all models include a mortality process based on low vitality and five of the models include some kind of mortality from physical disturbance (for instance, fire or a generic random disturbance intended to represent, e.g., wind-throw and biotic disturbance; Table 3). Classifying the models according to the relative importance of conceptually distinct mortality processes reveals markedly different hypotheses as to whether vitality or a physical disturbance is the primary cause of carbon turnover from mortality across global forests (Fig. 6) (Table 5: H4). Latitudinal variation in the dominant mortality process is limited (Fig. 6).
300

The mortality processes included in the TBMs have a limited ability to capture observed tree mortality attributed to drought. For drought-induced mortality, three of the six models (CABLE-POP, JULES, LPJmL) exhibit a substantially greater occurrence of mortality events at times and locations where such events have been reported in the literature, compared to a set of 10 randomly chosen times at each location (Table S5). All models showed some success in capturing dieback events using representations of processes that are conceptually consistent with drought-induced mortality (Table S5). However, the total percentage of observed events captured is very low, not exceeding 27%.
305

3.2 Future changes in τ under climate change

The TBMs considered in this study show substantial increases in biomass but divergent responses in τ over 2000-2099 under projected climate change (Fig. 7), which agrees with the findings of Friend et al. (2014) using an ensemble of simulations. Simulated changes in τ_{mort} are both positive and negative (Fig. 7c), but only ORCHIDEE projects an increase in τ_{mort} over the scenario period. LPJ-GUESS also stands out, displaying a strong decrease in τ_{mort} , despite the strong increase in overall τ . These changes in turnover time show high variability among regions and forest types (Fig. 8), and in several cases clearly follow forest type shifts (Fig. S10). In all the models, temporal variation in τ is predominantly associated with changes in mortality rather than phenology (Fig. 4b), consistent with intrinsic changes in mortality rate within forest type (MI_{MR}). The particular mechanisms driving the changes in turnover differ greatly between the models and embody most of those outlined in Table 1.
310
315

Substantial changes in mortality rates (MI_{MR}) over 2000-2085 are apparent for at least some forest types in five models (Figs. 8, S11-S16). For example, in temperate broadleaved and needleleaved forests three of the models show increases in vitality-related mortality (JULES, LPJ-GUESS, LPJmL) and one model shows a decrease followed by an increase (CABLE-POP). As described below, the reasons behind these changes differ among models.
320

In LPJmL, heat stress results in a substantial die-off at the boreal forest southern margin, triggering large, lagged increases in mortality rate due to self-thinning (also a vitality-based mechanism; Table 3) as the young forest regrows (Fig. S14e-h). The
325



330 heat-stress mortality rate declines with time as the PFT composition shifts towards temperate broadleaved deciduous trees, which in LPJmL are not subject to heat stress mortality. The substantial changes in mortality rates are thus characteristic of a large-scale dieback and recovery, but are unlikely to be representative of the long-term rates once the forest has recovered (see also Sitch et al., 2008). Mortality rates following full recovery from the transition are likely to differ from the pre-transition rates because mortality rates for some processes in LPJmL are PFT specific (MP_{MR}).

335 Increases in vitality-induced mortality in LPJ-GUESS (Fig. S13e-h) show how demographic shifts can result in a change in the mortality rate of a PFT, without any increased likelihood of individual tree death. As the climate warms the needleleaved evergreen PFTs begin to experience establishment failure, and the consequent shift of the age distribution towards larger tree sizes is manifested as an increase in the rate of background mortality of that PFT (likelihood of background mortality is a function of tree age in LPJ-GUESS). As larger trees die, the resulting space is colonised by the shade-intolerant broadleaved deciduous PFT, which is more vulnerable to vitality-induced mortality. Hence, much of the increase in vitality-based mortality is the outcome of, rather than the trigger for, a PFT shift towards a different forest type and an earlier successional stage (MP_{MR}). Thus, in both LPJmL and LPJ-GUESS, PFT shifts lead to substantial changes in τ through MP mechanisms (Table 5: H5), but in LPJmL PFT shifts are accelerated by increased mortality of established trees, whereas in LPJ-GUESS establishment failure drives a slower transition (Table 5: H6)

345 In JULES, increases in vitality-based mortality (Fig. S12e-h) are the result of ongoing PFT shifts under changing environmental conditions. The growth and loss of carbon due to competition is represented in one equation within JULES, with the most productive PFT being favoured. Changes in mortality rates are thus associated with shifts in forest type, but there are no processes to realise a long-term shift in mortality rates following MI-type mechanisms. Long-term mortality rate shifts can only be realised through MP-type mechanisms (Clark et al., 2011). Thus, JULES implicitly includes a version of hypothesis H5 (Table 5) in that the mortality rate under equilibrium with environmental conditions is independent of those conditions, except to the extent it changes functional composition.

350 CABLE-POP was run without dynamic vegetation, providing a clear demonstration of processes underlying the MI_{MR} mechanism. The model displays a transient reduction in temperate and needleleaved forest mortality rate in the first half of the 21st century (Fig. S11e-h) due to increasing NPP, which reduces vitality-induced mortality (Table 5: H7b). The increase in mortality rate towards the end of the 21st century appears to reflect strong warming reducing growth efficiency, possibly related to a temperature-induced reduction in carbon-use efficiency. The self-thinning component of vitality-based mortality increases throughout the simulation (not shown), as enhanced NPP leads to greater increments in crown size each year, following mechanism MS_{comp} (Table 5: H7a).



360 In contrast to mortality rate changes in temperate forests, none of the models show large increases in mortality rates across
tropical forests, and both LPJmL and ORCHIDEE show substantial decreases in mortality rates in these regions (Fig. 8). For
LPJmL (for which the process breakdown is available; Fig. S14a-c), this mortality rate decrease appears to be a result of
increased NPP reducing the likelihood of growth-efficiency mortality being triggered (Table 5: H7b). However, as all of the
models have similar formulations of vitality-based mortality (with the exception of JULES), it is notable that JULES, LPJ-
365 GUESS and SEIB-DGVM show small increases in vitality-induced mortality rates, alongside strong increases in NPP (Fig.
S17). We interpret these results to be further examples of increased mortality through accelerated resource competition between
trees (i.e. self-thinning; MS_{comp} , H7a); i.e., although the likelihood of death of the largest trees by vitality-based processes due
to environmental extremes may be reduced, turnover rates at the stand level may be maintained or increase as faster growth
accelerates competition.

370 Although the mortality (MI_{MR}) and forest-type-shift (MP) mechanisms are important drivers of changes in τ in the TBMs,
other mechanisms are also relevant in explaining the simulated responses of τ to environmental change. For instance, LPJ-
GUESS displays behaviour following $MI_{NPP,FS}$ (Fig. 8d); as NPP increases, a larger fraction of it is invested in wood (Fig. 3b),
increasing τ despite decreases in τ_{mort} (Fig. 8b,c). Mechanism $MI_{NPP,FS}$ occurs in all models except ORCHIDEE to varying
degrees (Fig. 3b) (Table 5: H8a), but CABLE-POP and ORCHIDEE tend more towards $MI_{NPP,F}$, which increases biomass with
375 no influence on τ (Table 5: H8b). LPJ-GUESS and LPJmL reduce their fraction of turnover due to roots more than the fraction
of turnover due to leaves (Fig. 3b). This appears to be a response of the functional-balance allocation approach (Sitch et al.,
2003; Smith et al., 2014) to increased water-use efficiency under elevated atmospheric CO_2 concentrations (MI_{RA}). In contrast,
despite encoding a functional-balance approach in which allocation is sensitive to moisture (Krinner et al., 2005), the allocation
scheme in ORCHIDEE results in a small increase in the fraction of carbon turnover through roots, perhaps driven by forest-
380 type shifts, and therefore corresponding to MP_{RA} .

4. Discussion and recommendations

A wide range of estimates of recent-historical and projected future carbon turnover time emerge from the TBM ensemble. Two
contrasting modes of simulated turnover response to changing environmental conditions were identified: (1) individual or
stand-level responses where internal physiology influences turnover in response to temperature, atmospheric CO_2
385 concentration, or other extrinsic drivers; and (2) population responses where shifts in species composition, age distribution,
etc. influenced forest composition or demography, with concomitant changes to turnover. The magnitude of individual, stand
and population responses varied across TBMs, as did the processes producing these responses. Of the possible mechanisms
governing changes in future τ and biomass stocks outlined in Table 1, only MI_{ST} and MP_{NPP} could not be clearly identified in
the TBM ensemble here. These differences in both modelled processes and emergent response arise because the key ecosystem



390 states and fluxes, and their relationships to environmental drivers, have been under-constrained by observations at regional
and global scales.

Based on the TBM ensemble, several emergent hypotheses (H1-H8) relating to both recent-historical and future carbon
turnover rates were identified (Table 5). Resolving the uncertainty around recent-historical and projected future large-scale
395 carbon turnover rates will require additional observational data, model development, and further exploration of these
hypotheses. In the following discussion, the state of science relating to each hypothesis is briefly reviewed and pathways for
testing the hypothesis, advancing understanding, and reducing TBM uncertainty are described.

4.1 The partitioning of turnover flux between soft and woody tissues (H1)

Even given firm constraints on biomass and NPP, both forms of hypothesis H1 (H1a and H1b, Table 5) would be possible,
400 necessitating direct constraints on either allocation or turnover rates for soft tissues. Plant trait databases provide numerous
observations of leaf longevity and specific leaf area (Kattge et al., 2011). Conversion of this information to typical values at
the PFT level should now be possible using species abundance information (e.g. Bruelheide et al., 2018) to appropriately
weight species-level data. Plasticity in plant behaviour, such as leaf shedding during drought or changing specific leaf area
under elevated atmospheric CO₂ concentrations (Medlyn et al., 2015), requires further investigation, however, as does the
405 influence of herbivory on leaf turnover, which is usually absent in TBM studies. Using observations to constrain reproductive
turnover is more challenging to address; observed investment in reproduction varies between species by up to several tens of
percent of NPP, and changes over a tree's lifecycle (Wenk and Falster, 2015). Yet the huge amount of information on seed
mass (Díaz et al., 2016) is not matched by similar information on fruit and flower mass and intervals between flowering.
Systematic sampling and data compilation efforts to populate knowledge gaps (Wenk and Falster, 2015) will likely be needed
410 to confidently move beyond the 10% of NPP assumption of Sitch et al. (2003) at the global scale.

The most striking disparity between models, however, is the fraction of carbon turned over by fine roots. Although some
studies have reported turnover times of many years (Matamala and Gonza, 2003), turnover times of around one year or less
are supported by meta-analyses for boreal, temperate and tropical forests (Brunner et al., 2013; Finér et al., 2011; Yuan and
415 Chen, 2010), but high methodological uncertainties persist due to inconsistent definitions of fine roots and difficulties in
measuring changes in below-ground tissues (Brunner et al., 2013; Finér et al., 2011). In addition, the same problems of scaling
observations across large areas for leaves also apply to roots. Assuming a turnover time of circa one year, fine root production
has been estimated to total a third of NPP (Jackson et al., 1997), a larger value than simulated by most of the TBMs herein.

420 Exudates may also be a substantial percentage of NPP in some ecosystems (Grayston et al., 1996). Conceptually, in TBMs,
they may currently be considered as implicit within either fine root allocation or root respiration. Given short turnover times,



425 either assumption is probably adequate as a first approximation, especially when combined with allocation schemes that can
capture environmentally driven changes (e.g. functional balance). On-going research, for instance at the current generation of
forest free-air CO₂ experiments (FACE; Norby et al., 2016), should provide improved understanding of response functions,
allowing better constraints of such responses (e.g. De Kauwe et al., 2014). Yet in the global scale simulations of the TBMs
herein, uncertainty in baseline below-ground turnover ranging from 6 to 37% of NPP dwarves the uncertainty in how such
investment will evolve under environmental change (Fig. 3).

4.2 The role of phenology versus mortality in driving spatial variation in τ (H2)

430 Much discussion has recently been devoted to potential changes in tree mortality rates and the resultant carbon cycle
implications (e.g. Adams et al., 2010; Anderegg et al., 2012; Bennett et al., 2015; McDowell et al., 2018). Whilst the results
of this study support the importance of mortality rates on determining τ , they also demonstrate that different strategies in
allocation to soft tissues are behind much of the spatial variation in τ in contemporary TBMs. In TBMs, phenological (and
often mortality) turnover rates are strongly tied to PFTs (e.g. Table S2), reflecting different functional strategies, making
simulation of the correct PFT distribution crucial to accurately determine τ .

435 Furthermore, it is not clear whether the prevailing PFT paradigm, based largely on leaf phenology, appropriately captures the
wider range of plant life-history strategies, which affect allocation of NPP and vulnerability to mortality, in trees in any given
forest type (Reich, 2014; Salguero-Gómez et al., 2016). Large trait databases (e.g. TRY; Kattge et al., 2011) and inventory
datasets (Brienen et al., 2015; Hember et al., 2016; Ruiz-Benito et al., 2016) can be leveraged to test this and diversification
440 of the strategies represented in TBMs, either through additional PFTs or flexible trait approaches (Langan et al., 2017; Pavlick
et al., 2013; Sakschewski et al., 2015; Scheiter et al., 2013), may be necessary.

New cross-walking techniques (Poulter et al., 2015) help to resolve the inconsistency between satellite landcover
classifications (e.g. ESA CCI; ESA, 2017) and PFTs simulated by TBMs, facilitating a standardised benchmarking processes
445 for PFT distributions. However, global tree, and thus PFT, distribution is an amalgamation of natural dynamics and forest
management activities. As large-scale forest management information is lacking, TBMs often simulate only the effect of
natural dynamics on forest properties. Accurately representing the effect of forest management across the globe, such as
recently developed for Europe (McGrath et al., 2015), will be crucial to simulating current PFT distributions and other forest
properties for the right reasons. Combining satellite landcover with inventory data will better capture forest management
450 practices along with finer details of PFT distributions that elude current landcover classifications (Schelhaas et al., 2018).
Hyperspectral remote sensing may also help provide greater fidelity in identifying different PFTs where reliable inventories
are lacking (Asner and Martin, 2016).



4.3 Woody biomass: Long turnover times or high C allocation? (H3)

455 Observations from tropical forest plots point towards τ_{mort} being underestimated in all TBMs herein (Fig. S9) and suggest that
an over-allocation to wood in these regions might be, to varying degrees, a common feature of TBMs. Because the carbon
460 allocated to wood in TBMs is a trade-off with respiration and soft-tissue demands, this indicates that the latter might be
underestimated. However, since increases in leaf area index or fine root mass per unit ground area provide a diminishing return
in terms of resource acquisition, it may be that understanding allocation to reproduction and defence that is key to balancing
tree carbon budgets. Efforts described in Section 4.1 will greatly assist in closing this knowledge gap regarding allocation;
465 however, H3 can be directly tested by strongly constraining τ_{mort} across all forests. The necessary information exists in forest
inventory and research plot data for all major forest types (Brienen et al., 2015; Carnicer et al., 2011; Hember et al., 2016;
Holzwarth et al., 2013; Lines et al., 2010; van Mantgem et al., 2009; Peng et al., 2011; Phillips et al., 2010), but this information
needs to be collated and standardised such that consistent comparisons across regions can be made. A comprehensive database
based on such data could be used to benchmark TBMs by biomass turnover and, for individual or cohort models, stem turnover.
470 Where possible, branch turnover flux, currently ignored in most TBMs, should also be assessed. If recently reported fluxes
approaching 50% of woody turnover (Marvin and Asner, 2016) are widespread and broadly supported, the implications would
propagate through the simulation of allocation and forest structure.

4.4 Processes causing tree mortality (H4)

470 To have accurate predictions in the context of global environmental change, mortality must be simulated for the right reasons,
resolving the very different hypotheses regarding the dominant form of tree death (Fig. 6). Fundamental to this effort will be
including process information at a level of complexity appropriate for the scale to be simulated. For instance, it may not be
necessary to simulate explicitly the dynamics of a pest that causes tree death if the resulting mortality is closely associated
with tree vitality. The TBMs herein combine a variety of mortality processes, which often bear a clear conceptual relation to
observed drivers of tree death (e.g. low vitality, large-scale disturbance, maximum age/height). That they yield such different
475 projections (Figs. 7, 8) is a result of challenges in both model parameterisation and conceptualisation. Forest inventories and
research plots may not give the proximate cause of death, but, assuming that woody growth is a good proxy for vitality (as in
e.g. Schumacher et al., 2006), many inventory protocols give enough information to constrain the vitality and background
processes outlined in Table 3. A first step is thus for modellers to further leverage these data to adapt and better constrain
existing approaches to simulating tree mortality.

480

Fully resolving H4 is likely to require inclusion of additional processes in TBMs, however, particularly large disturbances and
hydraulic failure. Whilst tree mortality from fire is explicitly included in many current TBMs (e.g. Table 3), tree mortality
from ephemeral insect and pathogen outbreaks, which, at least in some regions, might be similar in magnitude to tree mortality
from fire (Kautz et al., 2018) and liable to intensify with global warming (Seidl et al., 2017), is not explicitly simulated. Neither



485 are stand-replacing windthrow events, which are the main natural disturbance in parts of temperate and tropical forests
(Negrón-Juárez et al., 2018; Seidl et al., 2014). Comprehensive assessments of past and potential future impacts on forests due
to such disturbances requires a process-orientated modelling approach (Chen et al., 2018; Dietze and Matthes, 2014; Huang et
al., 2019; Landry et al., 2016), which remains highly challenging. However, using prescribed, spatially, and where possible
temporally, explicit disturbance fraction maps based on observations will help to improve simulations of carbon turnover
490 dynamics in current forests (Kautz et al., 2018; Pugh et al., 2019a). A first such map now exists for biotic disturbance for the
northern hemisphere (Kautz et al., 2017), but the underlying data are scarce in many regions. For windthrow, probability maps
do not currently exist at the global scale, but new generations of remote sensing products, building on the forest loss maps of
Hansen et al. (2013), offer hope that this information will gradually become available in the coming years (e.g. Curtis et al.,
2018; McDowell et al., 2015). Maximising the benefit from including such disturbances will, however, require TBMs to
495 explicitly track forest stand age, and indeed tree ages or sizes. TBMs which lump age/size classes will miss lagged sources or
sinks resulting from how temporal changes in disturbances rates affect forest demography (Pugh et al., 2019b).

Lastly, much recent research has centred on the cause of death during drought, whether this is hydraulic failure, carbon
starvation, phloem transport failure, or secondary biotic attack as a shortage of carbohydrate reduces the ability of the tree to
500 defend itself (Hartmann, 2015; Hartmann et al., 2018; McDowell et al., 2008; McDowell, 2011; Sevanto et al., 2014). Whilst
the latter three can all to some extent be related to vitality, hydraulic failure of the xylem transport system is conceptually
distinct and the latest evidence suggests that it plays a major role in many ecosystems (Anderegg et al., 2015, 2016; Hartmann,
2015; Liu et al., 2017; Rowland et al., 2015). It is especially relevant to τ_{mort} because hydraulic failure appears more likely to
occur in larger trees (Bennett et al., 2015; Rowland et al., 2015; Ryan et al., 2006), which hold the majority of biomass carbon
505 stocks, and whose death will create large canopy gaps for regeneration. There is currently no representation of hydraulic failure
incorporated within the TBMs here, however, several efforts to achieve this are on-going within the community (Eller et al.,
2019; Kennedy et al., 2019; Xu et al., 2016). Large-scale evaluation of these representations will benefit from compilations of
drought mortality events with increased event meta-data on cause of death, scale of the event and mortality rates (e.g.
Greenwood et al., 2017), alongside exact locations and site characteristics such as slope and soil type. Such meta-data will
510 help to minimise scale mismatches and better resolve contributory factors.

4.5 Response of τ to environmental change: PFT establishment rates (H5, H6)

Whilst changes in τ over the next few decades may result from mortality of existing trees, longer-term changes may result
from permanent shifts in mortality likelihood or from shifts towards plants with different characteristic mortality or
phenological turnover rates (i.e. life-history strategies) that better suit the new environment (Salguero-Gómez et al., 2016).
515 Such shifts have been detected in the Amazon region (Esquivel Muelbert et al., 2019) and in other taxa in Europe (Bowler et
al., 2017). The TBMs used here display both behaviours. Better understanding of tree mortality processes and thresholds (see



Section 4.4) will help identify the extent to which changes in turnover rates can occur without a shift in vegetation composition, however it is establishment which will govern the long-term response. Establishment in TBMs is generally based either on NPP or the abundance of mature trees, often within defined bioclimatic limits (Krinner et al., 2005; Sato et al., 2007; Sitch et al., 2003). These representations may be too simple because they exclude three important factors. First, existing climatic relationships for establishment may not hold under elevated atmospheric CO₂ concentrations because of alterations in seedling assimilation rates (Hattenschwiler and Korner, 2000; Würth et al., 1998). This situation may require additional experimental work in chambers or plots with perturbed conditions such as FACE (e.g. Norby et al., 2016) to determine whether a change in seedling assimilation rates is likely to lead to a vegetation composition shift, thus affecting τ via MP mechanisms. Second, the type of trees which establish is strongly affected by the light and moisture environment at the forest floor (Muscolo et al., 2014; Poorter et al., 2019) and likely interacts with CO₂ concentration (Hattenschwiler and Korner, 2000). Changing mortality rates and driving mechanisms will affect canopy gap sizes, gap formation rates, and the intensity of the gap-forming disturbance (i.e. is the understory also lost?) (Beckage et al., 2008), influencing the ratio of early successional to late successional trees, which is highly likely to affect τ_{mort} (MP mechanisms in Table 1). Thus, representations of forest demography and canopy gap dynamics may be necessary in order to prognostically simulate establishment under changing environmental conditions. Third, seed dispersal limits the speed at which species composition changes in response to changing environmental conditions, with many plant species unlikely to keep up with climate change (Corlett and Westcott, 2013) and some already lagging behind their climatic niche (e.g. Zhu et al., 2012). Furthermore, not all species have the same dispersal abilities, with early successional species having on average higher dispersal abilities than mid and late successional species (Meier et al., 2012). Considering these three factors may substantially increase TBM complexity, therefore exploratory work is needed to more thoroughly assess their potential importance and to further develop parsimonious and scale-appropriate algorithms which focus on the most influential components of these processes (e.g. Lehsten et al., 2019).

4.6 Impact of elevated atmospheric CO₂ concentration on mortality (H7)

Reduced rates of mortality due to elevated atmospheric CO₂ concentration (H7b) are conceptually included in five of the TBMs through the growth efficiency process (Table 3) and is evident in the overall response for two of them (Table 5). Such behaviour follows well-established leaf-level responses of photosynthesis and water-use efficiency to atmospheric CO₂ concentration, and is supported by detailed stand-level modelling (Liu et al., 2017), but is hard to verify with observations in mature trees (Walker et al., 2019). If trees expend their extra NPP on growing proportionally larger, thereby increasing their respiration demands, then the positive effect of enhanced NPP could be offset. Increased water-use efficiency under elevated CO₂ could also reduce mortality due to hydraulic failure (Liu et al., 2017), but none of the models herein capture that interaction (Section 4.4).



Increases in NPP are also linked to mortality through competition (Table 1; MS_{comp}). Higher growth rates will increase the rate of vitality-induced mortality in forest stands (Pretzsch et al., 2014), thus acting to reduce τ_{mort} . These relationships of tree size to stand density are very well established (Coomes and Allen, 2007; Enquist et al., 2009; Pretzsch, 2006; Westoby, 1984) and the process is included either directly, or via growth efficiency, in all of the TBMs herein (Table 3). This “self-thinning” process does not put a firm limit on stand biomass, as tree allometry means that large trees hold more biomass than a larger number of smaller trees covering the same area. However, it means that reductions in tree mortality rates during drought extremes due to increased vitality resulting from increased atmospheric CO_2 concentrations will be at least partially offset by increased mortality rates through stand dynamics if extra NPP is invested in growth. Where the balance lies will depend on the frequency and severity of drought events, the level of competition between individual trees for resources and the slope of the density versus size relationship, which is not well constrained across different forest compositions and age structures (Enquist et al., 2009; Pillet et al., 2018; Pretzsch, 2006). More extensive use of information from plot networks (e.g. Crowther et al., 2015; Liang et al., 2016; Brienens et al., 2015) could provide a relatively tight constraint on baseline mortality rates resulting from competition. Further, such data can be used for routine benchmarking of stand-level stem density vs biomass relationships in cohort and individual-based TBMs.

4.7 Allocation of extra resources: Wood or elsewhere? (H8)

Given the lack of constraint regarding allocation fractions under current conditions (H1, Section 4.1), that differences in the response of allocation to increased productivity exist between TBMs is perhaps unsurprising, with the models displaying behaviour following both $MI_{NPP,F}$ and $MI_{NPP,FS}$. Both hypotheses H8a and H8b are eminently plausible. If light and water/nutrient capture are already maximised then there is little advantage in further investment in leaves or fine roots, suggesting that allocation to these tissues should reach an effective limit. But, as with H3, whether the additional carbon is allocated preferentially to wood growth, or to rapid turnover items such as defence compounds, reproduction or exudates is unclear. Careful tracking of carbon in CO_2 enrichment experiments such as FACE will give answers for some ecosystems (Medlyn et al., 2015; Norby et al., 2016) and can be used to set initial bounds on behaviour. Model parameterisation across a broader range of ecosystems may require setting these experimental outcomes in the context of how productivity and allocation vary in observations of individual tree species across resource gradients (e.g. Tomlinson et al., 2012), or relating allocation strategies to genetic drivers (Blumstein et al., 2018). This is an extremely challenging aspect of TBM behaviour to constrain, but the assumption made has a substantial influence on simulated future τ and biomass stocks and should at least be clearly stated.

5 Conclusion

Baseline biomass carbon turnover times at the global scale are highly uncertain and this uncertainty is caused not just by mortality, but also by a range of mechanisms that affect allocation to, and turnover rates of, soft tissues. A focus primarily on



580 τ_{mort} , on the grounds that most of the biomass is held within the wood of trees is necessarily a static view of forests. In reality,
and in TBMs, forests are dynamic, their species composition and the allocation of carbon between different biomass
compartments responding to changes in their environment. Thus, constraining the current large uncertainty in overall woody
carbon turnover rates is crucial, but so too is accurately assessing the conditions which favour establishment of individual tree
types following mortality events, and quantifying for these individual tree types the characteristic mortality, allocation between
wood and soft tissues, and the turnover rates of these soft tissues.

585

It was not possible here to draw robust conclusions from the TBM simulations regarding likely changes of τ in different regions
or time periods. All of the behaviours discussed herein are plausible given the state of current knowledge. Testing the identified
model-based hypotheses will help to reduce both spatial and temporal uncertainty in τ . Although testing some of these
hypotheses will be challenging and require new fieldwork, significant progress can be made using existing knowledge and
590 data, particularly for H2, H3, H4 and H7a. Key to this effort will be ensuring a smooth interface between TBMs and
observations. This task requires efforts both to (1) compile and analyse observational data in ways that directly inform TBMs
and (2) design or modify TBMs to ensure that they are structurally capable of using those data. For instance, accurately
representing forest demography in TBMs is clearly central to simulating many of the important processes highlighted above,
but it also allows the TBM simulations to be directly compared to, and constrained by, inventory data (Fisher et al., 2018). In
595 some cases, confidence in TBMs may increase if they can simulate properties that are widely observed and can be used for
constraining model simulations, such as satellite reflectance values. It will be important to incorporate observational data
compilations into standardised benchmarking methods (e.g. Schaphoff et al., 2018), facilitating model evaluation and
improvement. Rather than painting a dispiriting picture, the divergence of TBM estimates of τ reflects the ingenuity of
scientists in the relatively data-poor world in which most TBM vegetation dynamics schemes were first developed. With the
600 enormous increase in observational data over the last two decades, there is great potential for rapid improvements.

Data and code availability

The model simulations described in this study can be accessed at <https://zenodo.org/communities/veg-turnover-comp/>. Code
for the analysis and figures in this study can be downloaded from https://github.com/pughtam/turnover_comp.git.

Author contribution

605 TAMP led the analysis and designed the modelling protocol. TAMP, JB, BB, VH, AH, JH, KZ, AR and HS contributed model
simulations. TAMP, TTR, SLS, and JS carried out the data analysis. TAMP, AA, SH, MK, BQ, TTR and SLS wrote the
manuscript. All authors commented on the manuscript.



Competing Interests

The authors declare that they have no conflict of interest.

610 Acknowledgements

The research in this article resulted from the workshop *Dynamic Global Vegetation Modelling: Towards a third generation*, held in Landskrona, Sweden, in May 2015, and funded by the Swedish Research Council FORMAS through a grant for the project Land Use Today and Tomorrow (Dnr. 211-2009-1682), and by the Strategic Research Areas BECC and MERGE. T.A.M.P. acknowledges support from the European Research Council under the European Union Horizon 2020 programme
615 (Grant 758873, TreeMort). T.A.M.P. and A.A. acknowledge support from European Union FP7 Grant LUC4C (Grant 603542), and the Helmholtz Association in its ATMO programme. J.B. was supported by the Centre National de la Recherche Scientifique (CNRS) of France through the program “Make Our Planet Great Again”. S.L.S. was supported by the U.S. Geological Survey Land Change Science Program. This is paper number 42 of the Birmingham Institute of Forest Research. David Galbraith is thanked for providing turnover times from tropical plots. Jon Sadler is thanked for advice on analysis, along
620 with Dominique Bachelet and Todd Hawbaker for their comments on an earlier version of the paper. Any use of trade, firm, or product names is for descriptive purposes only and does not imply endorsement by the U.S. Government.

References

- Adams, H. D., Macalady, A. K., Breshears, D. D., Allen, C. D., Stephenson, N. L., Saleska, S. R., Huxman, T. E., and
625 McDowell, N. G.: Climate-induced tree mortality: Earth system consequences, *Eos* (Washington, DC), 91(17), 153–154, <https://doi.org/10.1029/2010EO170003>, 2010.
- Adams, H. D., Williams, A. P., Xu, C., Rauscher, S. A., Jiang, X., and McDowell, N. G.: Empirical and process-based approaches to climate-induced forest mortality models., *Front. Plant Sci.*, 4, 438, <https://doi.org/10.3389/fpls.2013.00438>, 2013.
- Ahlström, A., Schurgers, G., Arneth, A., and Smith, B.: Robustness and uncertainty in terrestrial ecosystem carbon response
630 to CMIP5 climate change projections, *Environ. Res. Lett.*, 7(4), 044008, <https://doi.org/10.1088/1748-9326/7/4/044008>, 2012.
- Ahlström, A., Xia, J., Arneth, A., Luo, Y., and Smith, B.: Importance of vegetation dynamics for future terrestrial carbon cycling, *Environ. Res. Lett.*, 10(5), 054019, <https://doi.org/10.1088/1748-9326/10/5/054019>, 2015a.
- Ahlström, A., Raupach, M. R., Schurgers, G., Smith, B., Arneth, A., Jung, M., Reichstein, M., Canadell, J. G., Friedlingstein,
635 P., Jain, A. K., Kato, E., Poulter, B., Sitch, S., Stocker, B. D., Viovy, N., Wang, Y. P., Wiltshire, A., Zaehle, S., and Zeng, N.: The dominant role of semi-arid ecosystems in the trend and variability of the land CO₂ sink, *Science*, 6237, 895–899, <https://doi.org/10.1126/science.aaa1668>, 2015b.
- Allen, C. D., Macalady, A. K., Chenchouni, H., Bachelet, D., McDowell, N., Vennetier, M., Kitzberger, T., Rigling, A.,
640 Breshears, D. D., Hogg, E. H. (Ted), Gonzalez, P., Fensham, R., Zhang, Z., Castro, J., Demidova, N., Lim, J.-H., Allard, G., Running, S. W., Semerci, A., and Cobb, N.: A global overview of drought and heat-induced tree mortality reveals emerging climate change risks for forests, *For. Ecol. Manage.*, 259, 660–684, <https://doi.org/10.1016/j.foreco.2009.09.001>, 2010.
- Anderegg, W. R. L., Berry, J. A., Smith, D. D., Sperry, J. S., Anderegg, L. D. L., and Field, C. B.: The roles of hydraulic and



- 645 carbon stress in a widespread climate-induced forest die-off, *Proc. Natl. Acad. Sci.*, 109(1), 233–237, <https://doi.org/10.1073/pnas.1107891109>, 2012.
- Anderegg, W. R. L., Flint, A., Huang, C., Flint, L., Berry, J. A., Davis, F. W., Sperry, J. S., and Field, C. B.: Tree mortality predicted from drought-induced vascular damage, *Nat. Geosci.*, 8(May), 367–371, <https://doi.org/10.1038/ngeo2400>, 2015.
- 650 Anderegg, W. R. L., Klein, T., Bartlett, M., Sack, L., Pellegrini, A. F. A., Choat, B., and Jansen, S.: Meta-analysis reveals that hydraulic traits explain cross-species patterns of drought-induced tree mortality across the globe, *Proc. Natl. Acad. Sci. U. S. A.*, 113, 5024–5029, <https://doi.org/10.1073/pnas.1525678113>, 2016.
- Arneth, A., Harrison, S. P., Zaehle, S., Tsigaridis, K., Menon, S., Bartlein, P. J., Feichter, J., Korhola, A., Kulmala, M., O'Donnell, D., Schurgers, G., Sorvari, S., and Vesala, T.: Terrestrial biogeochemical feedbacks in the climate system, *Nat. Geosci.*, 3(8), 525–532, <https://doi.org/10.1038/ngeo905>, 2010.
- 655 Asner, G. P. and Martin, R. E.: Spectranomics: Emerging science and conservation opportunities at the interface of biodiversity and remote sensing, *Glob. Ecol. Conserv.*, 8, 212–219, <https://doi.org/10.1016/j.gecco.2016.09.010>, 2016.
- Ballantyne, A., Smith, W., Anderegg, W., Kauppi, P., Sarmiento, J., Tans, P., Shevliakova, E., Pan, Y., Poulter, B., Anav, A., Friedlingstein, P., Houghton, R., and Running, S.: Accelerating net terrestrial carbon uptake during the warming hiatus due to reduced respiration, *Nat. Clim. Chang.*, 7(2), 148–152, <https://doi.org/10.1038/nclimate3204>, 2017.
- 660 Beckage, B., Kloeppel, B. D., Yeakley, J. A., Taylor, S. F., and Coleman, D. C.: Differential Effects of Understory and Overstory Gaps on Tree Regeneration. *Journal of the Torrey Botanical Society* 135(1), 1–11, 2008.
- Bennett, A. C., McDowell, N. G., Allen, C. D., and Anderson-Teixeira, K. J.: Larger trees suffer most during drought in forests worldwide, *Nat. Plants*, 1, 15139, <https://doi.org/10.1038/nplants.2015.139>, 2015.
- Blumstein, M., Hopkins, R., Weston, D. J., Holbrook, N. M., and Richardson, A. D.: A Novel Approach to Quantifying the Drivers of Alternate Carbon Allocation Strategies in a Temperate, Deciduous Tree Species, *AGU Fall Meet. Abstr.*, 2018.
- 665 Bondeau, A., Smith, P. C., Zaehle, S., Schaphoff, S., Lucht, W., Cramer, W., Gerten, D., Lotze-Campen, H., Müller, C., Reichstein, M., and Smith, B.: Modelling the role of agriculture for the 20th century global terrestrial carbon balance, *Glob. Chang. Biol.*, 13(3), 679–706, <https://doi.org/10.1111/j.1365-2486.2006.01305.x>, 2007.
- Bowler, D. E., Hof, C., Haase, P., Kröncke, I., Schweiger, O., Adrian, R., Baert, L., Bauer, H.-G., Blick, T., Brooker, R. W., Dekoninck, W., Domisch, S., Eckmann, R., Hendrickx, F., Hickler, T., Klotz, S., Kraberg, A., Kühn, I., Matesanz, S., Meschede, A., Neumann, H., O'Hara, R., Russell, D. J., Sell, A. F., Sonnewald, M., Stoll, S., Sundermann, A., Tackenberg, O., Türkay, M., Valladares, F., van Herk, K., van Klink, R., Vermeulen, R., Voigtländer, K., Wagner, R., Welk, E., Wiemers, M., Wiltshire, K. H., and Böhning-Gaese, K.: Cross-realm assessment of climate change impacts on species' abundance trends, *Nat. Ecol. Evol.*, 1, 0067, <https://doi.org/10.1038/s41559-016-0067>, 2017.
- 670 Brando, P. M., Balch, J. K., Nepstad, D. C., Morton, D. C., Putz, F. E., Coe, M. T., Silvério, D., Macedo, M. N., Davidson, E. A., Nóbrega, C. C., Alencar, A., and Soares-Filho, B. S.: Abrupt increases in Amazonian tree mortality due to drought-fire interactions, *Proc. Natl. Acad. Sci. U. S. A.*, 111(17), 6347–6352, <https://doi.org/10.1073/pnas.1305499111>, 2014.
- 675 Brienen, R. J. W., Phillips, O. L., Feldpausch, T. R., Gloor, E., Baker, T. R., Lloyd, J., Lopez-Gonzalez, G., Monteagudo Mendoza, A., Malhi, Y., Lewis, S. L., Vásquez Martínez, R., Alexiades, M., Álvarez Dávila, E., Alvarez-Loayza, P., Andrade, A., Aragão, L. E. O. C., Araujo-Murakami, A., Arets, E. J. M. M., Arroyo, L., Aymard C., G. A., Bánki, O. S., Baraloto, C., Barroso, J. G., Bonal, D., Boot, R. G. A., Camargo, J. L., Castilho, C. V., Chama, V., Chao, K.-J., Chave, J., Comiskey, J. A., Cornejo Valverde, F., da Costa, L., De Oliveira, E. A., Di Fiore, A., Erwin, T. L., Fauset, S., Forsthofer, M., Galbraith, D. R., Grahame, E. S., Groot, N. E., Hérault, B., Higuchi, N., Honorio C., E., Keeling, H., Killeen, T. J., Laurance, W. F., Laurance, S., Licona, J.-C., Magnussen, W. E., Marimon, B. S., Marimon-Junior, B. H., Mendoza, C., Neill, D. A., Nogueira, E. M., Núñez, P., Pallqui Camacho, N. C., Parada, A., Pardo, G., Peacock, J., Peña-Claros, M., Pickavance, G. C., Pitman, N. C. A., Poorter, L., Prieto, A., Quesada, C. A., Ramírez, F., Ramírez-Angulo, H., Restrepo, Z., Roopsind, A., Rudas, A., Salomão, R. P., Schwarz, M., Silva, N., Silva-Espejo, J. E., Silveira, M., Stropp, J., Talbot, J., ter Steege, H., Teran-Aguilar, J., Terborgh, J., Thomas-Caesar, R., Toledo, M., Torello-Raventos, M., Umetsu, R. K., van der Heijden, G. M. F., van der Hout, P., Guimarães Vieira, I., Vieira, S. A., Vilanova, E., Vos, V., and Zagt, R. J.: Plot data from: “Long-term decline of the Amazon carbon sink,” https://doi.org/10.5521/forestplots.net/2014_4, 2014.
- 680 Brienen, R. J. W., Phillips, O. L., Feldpausch, T. R., Gloor, E., Baker, T. R., Lloyd, J., Lopez-Gonzales, G., Monteagudo-Mendoza, A., Malhi, Y., Lewis, S. L., Vásquez Martínez, R., Alexiades, M., Álvarez Dávila, E., Alvarez-Loayza, P., Andrade, A., Aragão, L. E. O. C., Araujo-Murakami, A., Arets, E. J. M. M., Arroyo, L., Aymard C., G. A., Bánki, O. S., Baraloto, C., Barroso, J., Bonal, D., Boot, R. G. A., Camargo, J. L. C., Castilho, C. V., Chama, V., Chao, K. J., Chave, J.,



- 695 Comiskey, J. A., Cornejo Valverde, F., da Costa, L., de Oliveira, E. A., Di Fiore, A., Erwin, T. L., Fauset, S., Forsthofer, M., Galbraith, D. R., Grahame, E. S., Groot, N., Hérault, B., Higuchi, N., Honorio Coronado, E. N., Keeling, H., Killeen, T. J., Laurance, W. F., Laurance, S., Licona, J., Magnussen, W. E., Marimon, B. S., Marimon-Junior, B. H., Mendoza, C., Neill, D. A., Nogueira, E. M., Núñez, P., Pallqui Camacho, N. C., Parada, A., Pardo-Molina, G., Peacock, J., Peña-Claros, M., Pickavance, G. C., Pitman, N. C. A., Poorter, L., Prieto, A., Quesada, C. A., Ramírez, F., Ramírez-Angulo, H., Restrepo, Z., Roopsind, A., Rudas, A., Salomão, R. P., Schwarz, M., Silva, N., Silva-Espejo, J. E., Silveira, M., Stropp, J., Talbot, J., ter Steege, H., Teran-Aguilar, J., Terborgh, J., Thomas-Caesar, R., Toledo, M., Torello-Raventos, M., Umetsu, R. K., van der Heijden, G. M. F., van der Hout, P., Guimarães Vieira, I. C., Vieira, S. A., Vilanova, E., Vos, V. A., and Zagt, R. J.: Long-term decline of the Amazon carbon sink, *Nature*, 519(7543), 344–348, <https://doi.org/10.1038/nature14283>, 2015.
- 700
- 705 Bruelheide, H., Dengler, J., Purschke, O., Lenoir, J., Jiménez-Alfaro, B., Hennekens, S. M., Botta-Dukát, Z., Chytrý, M., Field, R., Jansen, F., Kattge, J., Pillar, V. D., Schrod, F., Mahecha, M. D., Peet, R. K., Sandel, B., van Bodegom, P., Altman, J., Alvarez-Dávila, E., Arfin Khan, M. A. S., Attorre, F., Aubin, I., Baraloto, C., Barroso, J. G., Bauters, M., Bergmeier, E., Biurrun, I., Bjorkman, A. D., Blonder, B., Čarni, A., Cayuela, L., Černý, T., Cornelissen, J. H. C., Craven, D., Dainese, M., Derroire, G., De Sanctis, M., Díaz, S., Doležal, J., Farfan-Rios, W., Feldpausch, T. R., Fenton, N. J., Garnier, E., Guerin, G. R., Gutiérrez, A. G., Haider, S., Hattab, T., Henry, G., Hérault, B., Higuchi, P., Hölzel, N., Homeier, J., Jentsch, A., Jürgens, N., Kaçki, Z., Karger, D. N., Kessler, M., Kleyer, M., Knollová, I., Korolyuk, A. Y., Kühn, I., Laughlin, D. C., Lens, F., Loos, J., Louault, F., Lyubenova, M. I., Malhi, Y., Marcenò, C., Mencuccini, M., Müller, J. V., Munzinger, J., Myers-Smith, I. H., Neill, D. A., Niinemets, Ü., Orwin, K. H., Ozinga, W. A., Penuelas, J., Pérez-Haase, A., Petřík, P., Phillips, O. L., Pärtel, M., Reich, P. B., Römermann, C., Rodrigues, A. V., Sabatini, F. M., Sardans, J., Schmidt, M., Seidler, G., Silva Espejo, J. E., Silveira, M., Smyth, A., Sporb, M., Svenning, J.-C., Tang, Z., Thomas, R., Tsiripidis, I., Vassilev, K., Violle, C., Virtanen, R., Weiher, E., Welk, E., Wesche, K., Winter, M., Wirth, C., and Jandt, U.: Global trait–environment relationships of plant communities, *Nat. Ecol. Evol.*, 2(12), 1906–1917, <https://doi.org/10.1038/s41559-018-0699-8>, 2018.
- 710
- 715 Brunner, I., Bakker, M. R., Björk, R. G., Hirano, Y., Lukac, M., Aranda, X., Børja, I., Eldhuset, T. D., Helmisaari, H. S., Jourdan, C., Konôpka, B., López, B. C., Miguel Pérez, C., Persson, H., and Ostonen, I.: Fine-root turnover rates of European forests revisited: An analysis of data from sequential coring and ingrowth cores, *Plant Soil*, 362(1–2), 357–372, <https://doi.org/10.1007/s11104-012-1313-5>, 2013.
- 720 Bugmann, H. and Bigler, C.: Will the CO₂ fertilization effect in forests be offset by reduced tree longevity?, *Oecologia*, 165, 533–544, <https://doi.org/10.1007/s00442-010-1837-4>, 2011.
- 725 Carnicer, J., Coll, M., Ninyerola, M., Pons, X., Sánchez, G., and Peñuelas, J.: Widespread crown condition decline, food web disruption, and amplified tree mortality with increased climate change-type drought, *Proc. Natl. Acad. Sci.*, 108(4), 1474–1478, <https://doi.org/10.1073/pnas.1010070108>, 2011.
- 730 Carvalhais, N., Forkel, M., Khomik, M., Bellarby, J., Jung, M., Migliavacca, M., Mingquan, M., Saatchi, S., Santoro, M., Thurner, M., Weber, U., Ahrens, B., Beer, C., Cescatti, A., Randerson, J. T., and Reichstein, M.: Global covariation of carbon turnover times with climate in terrestrial ecosystems, *Nature*, 514(7521), 213–217, <https://doi.org/10.1038/nature13731>, 2014.
- 735 Chen, Y., Gardiner, B., Pasztor, F., Blennow, K., Ryder, J., Valade, A., Naudts, K., Otto, J., Mcgrath, M. J., Planque, C., and Luysaert, S.: Simulating damage for wind storms in the land surface model ORCHIDEE-CAN (revision 4262), *Geosci. Model Dev.*, 11, 771–791, <https://doi.org/10.5194/gmd-11-771-2018>, 2018.
- 740 Ciais, P., Sabine, C., Bala, G., Bopp, L., Brovkin, V., Canadell, J., Chhabra, A., DeFries, R., Galloway, J., Heimann, M., Jones, C., Le Quéré, C., Myneni, R. B., Piao, S., and Thornton, P.: Carbon and other biogeochemical cycles, in *Climate Change 2013: The Physical Science Basis. Contribution of Working Group I to the Fifth Assessment Report of the Intergovernmental Panel on Climate Change*, edited by T. F. Stocker, D. Qin, G.-K. Plattner, M. Tignor, S. K. Allen, J. Boschung, A. Nauels, Y. Xia, V. Bex, and P. M. Midgley, pp. 465–570, Cambridge University Press, Cambridge, United Kingdom and New York, NY, USA., 2013.
- Clark, D. B., Mercado, L. M., Sitch, S., Jones, C. D., Gedney, N., Best, M. J., Pryor, M., Rooney, G. G., Essery, R. L. H., Blyth, E., Boucher, O., Harding, R. J., Huntingford, C., and Cox, P. M.: The Joint UK Land Environment Simulator (JULES), model description – Part 2: Carbon fluxes and vegetation dynamics, *Geosci. Model Dev.*, 4(3), 701–722, <https://doi.org/10.5194/gmd-4-701-2011>, 2011.



- 745 Coomes, D. A. and Allen, R. B.: Mortality and tree-size distributions in natural mixed-age forests, *J. Ecol.*, 95(1), 27–40, <https://doi.org/10.1111/j.1365-2745.2006.01179.x>, 2007.
- Corlett, R. T. and Westcott, D. A.: Will plant movements keep up with climate change?, *Trends Ecol. Evol.*, 28(8), 482–488, <https://doi.org/10.1016/j.tree.2013.04.003>, 2013.
- 750 Cramer, W., Kicklighter, D. W., Bondeau, A., Moore III, B., Churkina, G., Nemry, B., Ruimy, A., Schloss, A. L., and The Participants of the Potsdam NPP Model Intercomparison: Comparing global models of terrestrial net primary productivity (NPP): overview and key results, *Glob. Chang. Biol.*, 5(1), 1–15, <https://doi.org/10.1046/j.1365-2486.1999.00009.x>, 1999.
- Crowther, T. W., Glick, H. B., Covey, K. R., Bettigole, C., Maynard, D. S., Thomas, S. M., Smith, J. R., Hintler, G., Duguid, M. C., Amatulli, G., Tuanmu, M.-N., Jetz, W., Salas, C., Stam, C., Piotto, D., Tavani, R., Green, S., Bruce, G., Williams, S. J., Wiser, S. K., Huber, M. O., Hengeveld, G. M., Nabuurs, G.-J., Tikhonova, E., Borchardt, P., Li, C.-F., Powrie, L. W., Fischer, M., Hemp, A., Homeier, J., Cho, P., Vibrans, A. C., Umunay, P. M., Piao, S. L., Rowe, C. W., Ashton, M. S., 755 Crane, P. R., and Bradford, M. A.: Mapping tree density at a global scale, *Nature*, 525, 201–205, <https://doi.org/10.1038/nature14967>, 2015.
- Curtis, P. G., Slay, C. M., Harris, N. L., Tyukavina, A., and Hansen, M. C.: Classifying drivers of global forest loss, *Science*, 1111, 1108–1111, <https://doi.org/10.1126/science.aau3445>, 2018.
- 760 De Kauwe, M. G., Medlyn, B. E., Zaehle, S., Walker, A. P., Dietze, M. C., Wang, Y.-P., Luo, Y., Jain, A. K., El-Masri, B., Hickler, T., Wårlind, D., Weng, E., Parton, W. J., Thornton, P. E., Wang, S., Prentice, I. C., Asao, S., Smith, B., McCarthy, H. R., Iversen, C. M., Hanson, P. J., Warren, J. M., Oren, R., and Norby, R. J.: Where does the carbon go? A model–data intercomparison of vegetation carbon allocation and turnover processes at two temperate forest free-air CO₂ enrichment sites, *New Phytol.*, 203, 883–899, <https://doi.org/10.1111/nph.12847>, 2014.
- 765 Díaz, S., Kattge, J., Cornelissen, J. H. C., Wright, I. J., Lavorel, S., Dray, S., Reu, B., Kleyer, M., Wirth, C., Prentice, I. C., Garnier, E., Bönsch, G., Westoby, M., Poorter, H., Reich, P. B., Moles, A. T., Dickie, J., Gillison, A. N., Zanne, A. E., Chave, J., Wright, S. J., Sheremet'ev, S. N., Jactel, H., Baraloto, C., Cerabolini, B., Pierce, S., Shipley, B., Kirkup, D., Casanoves, F., Joswig, J. S., Günther, A., Falczuk, V., Rüger, N., Mahecha, M. D., and Gorné, L. D.: The global spectrum of plant form and function, *Nature*, 529(7585), 167–171, <https://doi.org/10.1038/nature16489>, 2016.
- 770 Dietze, M. C. and Matthes, J. H.: A general ecophysiological framework for modelling the impact of pests and pathogens on forest ecosystems, *Ecol. Lett.*, 17(11), 1418–1426, <https://doi.org/10.1111/ele.12345>, 2014.
- Eller, C.B., Rowland, L., Mencuccini, M., Rosas, T., Williams, K., Harper, A., Medlyn, B. E., Wagner, Y., Klein, T., Teodoro, G. S., Oliveira, R. S., Matos, I. S., Rosado, B. H. P., Fuchs, K., Wohlfahrt, G., Montagnani, L., Meir, P., Sitch, S., Cox, P. M.: Stomatal optimisation based on xylem hydraulics (SOX) improves land surface model simulation of vegetation responses to climate, *New Phytologist*, accepted manuscript, <https://doi.org/10.1111/nph.16419>, 2020.
- 775 Enquist, B. J., West, G. B., and Brown, J. H.: Extensions and evaluations of a general quantitative theory of forest structure and dynamics., *Proc. Natl. Acad. Sci. U. S. A.*, 106(17), 7046–7051, <https://doi.org/10.1073/pnas.0812303106>, 2009.
- Erb, K.-H., Fetzel, T., Plutzer, C., Kastner, T., Lauk, C., Mayer, A., Niedertscheider, M., Körner, C., and Haberl, H.: Biomass turnover time in terrestrial ecosystems halved by land use, *Nat. Geosci.*, 9(9), 674–678, <https://doi.org/10.1038/ngeo2782>, 2016.
- 780 ESA: ESA CCI Land Cover dataset (v 2.0.7), [online] Available from: <http://maps.elie.ucl.ac.be/CCI/viewer/> (Accessed 29 June 2017), 2017.
- Esquivel-Muelbert, A., Baker, T. R., Dexter, K. G., Lewis, S. L., Brienen, R. J. W., Feldpausch, T. R., Lloyd, J., Monteagudo-Mendoza, A., Arroyo, L., Álvarez-Dávila, E., Higuchi, N., Marimon, B. S., Marimon-Junior, B. H., Silveira, M., Vilanova, E., Gloor, E., Malhi, Y., Chave, J., Barlow, J., Bonal, D., Davila Cardozo, N., Erwin, T., Fauset, S., Hérault, B., Laurance, S., Poorter, L., Qie, L., Stahl, C., Sullivan, M. J. P., ter Steege, H., Vos, V. A., Zuidema, P. A., Almeida, E., Almeida de 785 Oliveira, E., Andrade, A., Vieira, S. A., Aragão, L., Araujo-Murakami, A., Arets, E., Aymard, C., G. A., Baraloto, C., Barbosa Camargo, P., Barroso, J. G., Bongers, F., Boot, R., Camargo, J. L., Castro, W., Chama Moscoso, V., Comiskey, J., Cornejo Valverde, F., Lola da Costa, A. C., del Aguila Pasquel, J., Di Fiore, A., Fernanda Duque, L., Elias, F., Engel, J., Flores Lampazo, G., Galbraith, D., Herrera Fernández, R., Honorio Coronado, E., Hubau, W., Jimenez-Rojas, E., Lima, A. J. N., Umetsu, R. K., Laurance, W., Lopez-Gonzalez, G., Lovejoy, T., Aurelio Melo Cruz, O., Morandi, P. S., Neill, D., Núñez Vargas, P., Pallqui Camacho, N. C., Parada Gutierrez, A., Pardo, G., Peacock, J., Peña-Claros, M., Peñuela-Mora, M. C., Petronelli, P., Pickavance, G. C., Pitman, N., Prieto, A., Quesada, C., Ramírez-Angulo, H., Réjou-Méchain, M., Restrepo Correa, Z., Roopsind, A., Rudas, A., Salomão, R., Silva, N., Silva Espejo, J., Singh, J., Stropp, J., Terborgh,



- 795 J., Thomas, R., Toledo, M., Torres-Lezama, A., Valenzuela Gamarra, L., van de Meer, P. J., van der Heijden, G., van der Hout, P., Vasquez Martinez, R., Vela, C., Vieira, I. C. G., and Phillips, O. L.: Compositional response of Amazon forests to climate change, *Glob. Chang. Biol.*, 25, 39–56, <https://doi.org/10.1111/gcb.14413>, 2019.
- Finér, L., Ohashi, M., Noguchi, K., and Hirano, Y.: Fine root production and turnover in forest ecosystems in relation to stand and environmental characteristics, *For. Ecol. Manage.*, 262(11), 2008–2023, <https://doi.org/10.1016/j.foreco.2011.08.042>, 2011.
- 800 Fisher, R. A., Koven, C. D., Anderegg, W. R. L., Christoffersen, B. O., Dietze, M. C., Farrior, C. E., Holm, J. A., Hurtt, G. C., Knox, R. G., Lawrence, P. J., Lichstein, J. W., Longo, M., Matheny, A. M., Medvigy, D., Muller-Landau, H. C., Powell, T. L., Serbin, S. P., Sato, H., Shuman, J. K., Smith, B., Trugman, A. T., Viskari, T., Verbeeck, H., Weng, E., Xu, C., Xu, X., Zhang, T., and Moorcroft, P. R.: Vegetation demographics in Earth System Models: A review of progress and priorities, *Glob. Chang. Biol.*, 24, 35–54, <https://doi.org/10.1111/gcb.13910>, 2018.
- 805 Franklin, J. F., Shugart, H. H., and Harmon, M. E.: Tree death as an ecological process: The causes, consequences, and variability of tree mortality, *Bioscience*, 37(8), 550–556, <https://doi.org/10.2307/1310665>, 1987.
- Franklin, O., Johansson, J., Dewar, R. C., Dieckmann, U., McMurtrie, R. E., Brännström, Å., and Dybzinski, R.: Modeling carbon allocation in trees: A search for principles, *Tree Physiol.*, 32, 648–666, <https://doi.org/10.1093/treephys/tpr138>, 2012.
- 810 Friedlingstein, P., Meinshausen, M., Arora, V. K., Jones, C. D., Anav, A., Liddicoat, S. K., and Knutti, R.: Uncertainties in CMIP5 climate projections due to carbon cycle feedbacks, *J. Clim.*, 27(2), 511–526, <https://doi.org/10.1175/JCLI-D-12-00579.1>, 2014.
- Friend, A. D., Lucht, W., Rademacher, T. T., Keribin, R., Betts, R., Cadule, P., Ciais, P., Clark, D. B., Dankers, R., Falloon, P. D., Ito, A., Kahana, R., Kleidon, A., Lomas, M. R., Nishina, K., Ostberg, S., Pavlick, R., Peylin, P., Schaphoff, S., 815 Vuichard, N., Warszawski, L., Wiltshire, A., and Woodward, F. I.: Carbon residence time dominates uncertainty in terrestrial vegetation responses to future climate and atmospheric CO₂, *Proc. Natl. Acad. Sci. U. S. A.*, 111, 3280–3285, <https://doi.org/10.1073/pnas.1222477110>, 2014.
- Galbraith, D., Malhi, Y., Affum-Baffoe, K., Castanho, A. D. A., Doughty, C. E., Fisher, R. A., Lewis, S. L., Peh, K. S.-H., Phillips, O. L., Quesada, C. A., Sonké, B. and Lloyd, J.: Residence times of woody biomass in tropical forests, *Plant Ecol. Divers.*, 6(1), 139–157, <https://doi.org/10.1080/17550874.2013.770578>, 2013.
- 820 Grayston, S. J., Vaughan, D., and Jones, D.: Rhizosphere carbon flow in trees, in comparison with annual plants: the importance of root exudation and its impact on microbial activity and nutrient availability, *Appl. Soil Ecol.*, 5, 29–56, [https://doi.org/10.1016/S0929-1393\(96\)00126-6](https://doi.org/10.1016/S0929-1393(96)00126-6), 1996.
- Greenwood, S., Ruiz-Benito, P., Martinez-Vilalta, J., Lloret, F., Kitzberger, T., Allen, C. D., Fensham, R., Laughlin, D. C., 825 Kattge, J., Bönisch, G., Kraft, N. J. B., and Jump, A. S.: Tree mortality across biomes is promoted by drought intensity, lower wood density and higher specific leaf area, *Ecol. Lett.*, 20, 539–553, <https://doi.org/10.1111/ele.12748>, 2017.
- Hansen, M. C., Potapov, P. V., Moore, R., Hancher, M., Turubanova, S. A., Tyukavina, A., Thau, D., Stehman, S. V., Goetz, S. J., Loveland, T. R., Kommareddy, A., Egorov, A., Chini, L., Justice, C. O., and Townshend, J. R. G.: High-resolution global maps of 21st-century forest cover change., *Science*, 342, 850–853, <https://doi.org/10.1126/science.1244693>, 2013.
- 830 Hantson, S., Arneth, A., Harrison, S. P., Kelley, D. I., Prentice, I. C., Rabin, S. S., Archibald, S., Mouillot, F., Arnold, S. R., Artaxo, P., Bachelet, D., Ciais, P., Forrest, M., Friedlingstein, P., Hickler, T., Kaplan, J. O., Kloster, S., Knorr, W., Lasslop, G., Li, F., Mangeon, S., Melton, J. R., Meyn, A., Sitch, S., Spessa, A., van der Werf, G. R., Voulgarakis, A., and Yue, C.: The status and challenge of global fire modelling, *Biogeosciences*, 13(11), 3359–3375, <https://doi.org/10.5194/bg-13-3359-2016>, 2016.
- 835 Hartmann, H.: Carbon starvation during drought-induced tree mortality – are we chasing a myth?, *J. Plant Hydraul.*, 2, 1–5, <https://doi.org/10.20870/jph.2015.e005>, 2015.
- Hartmann, H., Moura, C. F., Anderegg, W. R. L., Ruehr, N. K., Salmon, Y., Allen, C. D., Arndt, S. K., Breshears, D. D., Davi, H., Galbraith, D., Ruthrof, K. X., Wunder, J., Adams, H. D., Bloemen, J., Cailleret, M., Cobb, R., Gessler, A., Grams, T. E. E., Jansen, S., Kautz, M., Lloret, F., and O’Brien, M.: Research frontiers for improving our understanding of drought- 840 induced tree and forest mortality, *New Phytol.*, 218, 15–28, <https://doi.org/10.1111/nph.15048>, 2018.
- Hattenschwiler, S. and Körner, C.: Tree seedling responses to in situ CO₂-enrichment differ among species and depend on understorey light availability, *Glob. Chang. Biol.*, 6(2), 213–226, <https://doi.org/10.1046/j.1365-2486.2000.00301.x>, 2000.
- Haverd, V., Smith, B., Nieradzic, L. P., and Briggs, P. R.: A stand-alone tree demography and landscape structure module for



- 845 Earth system models: Integration with inventory data from temperate and boreal forests, *Biogeosciences*, 11, 4039–4055, <https://doi.org/10.5194/bg-11-4039-2014>, 2014.
- Haverd, V., Smith, B., Nieradzik, L., Briggs, P. R., Woodgate, W., Trudinger, C. M., Canadell, J. G., and Cuntz, M.: A new version of the CABLE land surface model (Subversion revision r4601) incorporating land use and land cover change, woody vegetation demography, and a novel optimisation-based approach to plant coordination of photosynthesis, *Geosci. Model Dev.*, 11, 2995–3026, <https://doi.org/10.5194/gmd-11-2995-2018>, 2018.
- 850 Hember, R. A., Kurz, W. A., and Coops, N. C.: Relationships between individual-tree mortality and water-balance variables indicate positive trends in water stress-induced tree mortality across North America, *Glob. Chang. Biol.*, 23, 1691–1710, <https://doi.org/10.1111/gcb.13428>, 2016.
- Hempel, S., Frieler, K., Warszawski, L., Schewe, J., and Piontek, F.: A trend-preserving bias correction – The ISI-MIP approach, *Earth Syst. Dyn.*, 4, 219–236, <https://doi.org/10.5194/esd-4-219-2013>, 2013.
- 855 Hickler, T., Prentice, I. C., Smith, B., Sykes, M. T., and Zaehle, S.: Implementing plant hydraulic architecture within the LPJ Dynamic Global Vegetation Model, *Glob. Ecol. Biogeogr.*, 15, 567–577, <https://doi.org/10.1111/j.1466-8238.2006.00254.x>, 2006.
- Holzwarth, F., Kahl, A., Bauhus, J., and Wirth, C.: Many ways to die – partitioning tree mortality dynamics in a near-natural mixed deciduous forest, *J. Ecol.*, 101, 220–230, <https://doi.org/10.1111/1365-2745.12015>, 2013.
- 860 Huang, J., Kautz, M., Trowbridge, A. M., Hammerbacher, A., Raffa, K. F., Adams, H. D., Goodsman, D. W., Xu, C., Meddens, A., J. H., Kandasamy, D., Gershenson, J., Seidl, R., and Hartmann, H.: Tree defence and bark beetles in a drying world: carbon partitioning, functioning and modelling, *New Phytol.*, 225, 26–36, <https://doi.org/10.1111/nph.16173>, 2019.
- Jackson, R. B., Mooney, H. A., and Schulze, E.-D.: A global budget for fine root biomass, surface area, and nutrient contents, *Proc. Natl. Acad. Sci. U. S. A.*, 94(July), 7362–7366, <https://doi.org/10.1073/pnas.94.14.7362>, 1997.
- 865 Johnson, M. O., Galbraith, D., Gloor, M., De Deurwaerder, H., Guimberteau, M., Rammig, A., Thonicke, K., Verbeeck, H., von Randow, C., Monteagudo, A., Phillips, O. L., Brienen, R. J. W., Feldpausch, T. R., Lopez Gonzalez, G., Fauset, S., Quesada, C. A., Christoffersen, B., Ciais, P., Sampaio, G., Kruijt, B., Meir, P., Moorcroft, P., Zhang, K., Alvarez-Davila, E., Alves de Oliveira, A., Amaral, I., Andrade, A., Aragao, L. E. O. C., Araujo-Murakami, A., Arets, E. J. M. M., Arroyo, L., Aymard, G. A., Baraloto, C., Barroso, J., Bonal, D., Boot, R., Camargo, J., Chave, J., Cogollo, A., Cornejo Valverde, F., Lola da Costa, A. C., Di Fiore, A., Ferreira, L., Higuchi, N., Honorio, E. N., Killeen, T. J., Laurance, S. G., Laurance, W. F., Licona, J., Lovejoy, T., Malhi, Y., Marimon, B., Marimon Junior, B. H., Matos, D. C. L., Mendoza, C., Neill, D. A., Pardo, G., Peña-Claro, M., Pitman, N. C. A., Poorter, L., Prieto, A., Ramirez-Angulo, H., Roopsind, A., Rudas, A., Salomao, R. P., Silveira, M., Stropp, J., Ter Steege, H., Terborgh, J., Thomas, R., Toledo, M., Torres-Lezama, A., van der Heijden, G. M. F., Vasquez, R., Guimarães Vieira, I. C., Vilanova, E., Vos, V. A., and Baker, T. B.: Variation in stem mortality rates determines patterns of aboveground biomass in Amazonian forests: implications for dynamic global vegetation models, *Glob. Chang. Biol.*, 22(12), 3996–4013, <https://doi.org/10.1111/gcb.13315>, 2016.
- 875 Jones, C., Robertson, E., Arora, V., Friedlingstein, P., Shevliakova, E., Bopp, L., Brovkin, V., Hajima, T., Kato, E., Kawamiya, M., Liddicoat, S., Lindsay, K., Reick, C. H., Roelandt, C., Segschneider, J., and Tjiputra, J.: Twenty-first-century compatible CO₂ emissions and airborne fraction simulated by CMIP5 Earth system models under four representative concentration pathways, *J. Clim.*, 26(13), 4398–4413, <https://doi.org/10.1175/JCLI-D-12-00554.1>, 2013.
- 880 Kattge, J., Díaz, S., Lavorel, S., Prentice, I. C., Leadley, P., Bönisch, G., Garnier, E., Westoby, M., Reich, P. B., Wright, I. J., Cornelissen, J. H. C., Violle, C., Harrison, S. P., Van Bodegom, P. M., Reichstein, M., Enquist, B. J., Soudzilovskaia, N. A., Ackerly, D. D., Anand, M., Atkin, O., Bahn, M., Baker, T. R., Baldocchi, D., Bekker, R., Blanco, C. C., Blonder, B., Bond, W. J., Bradstock, R., Bunker, D. E., Casanoves, F., Cavender-Bares, J., Chambers, J. Q., Chapin III, F. S., Chave, J., Coomes, D., Comwell, W. K., Craine, J. M., Dobrin, B. H., Duarte, L., Durka, W., Elser, J., Esser, G., Estiarte, M., Fagan, W. F., Fang, J., Fernández-Méndez, F., Fidelis, A., Finegan, B., Flores, O., Ford, H., Frank, D., Freschet, G. T., Fyllas, N. M., Gallagher, R. V., Green, W. A., Gutierrez, A. G., Hickler, T., Higgins, S. I., Hodgson, J. G., Jalili, A., Jansen, S., Joly, C. A., Kerkhoff, A. J., Kirkup, D., Kitajima, K., Kleyer, M., Klotz, S., Knops, J. M. H., Kramer, K., Kühn, I., Kurokawa, H., Laughlin, D., Lee, T. D., Leishman, M., Lens, F., Lenz, T., Lewis, S. L., Lloyd, J., Llusià, J., Louault, F., Ma, S., Mahecha, M. D., Manning, P., Massad, T., Medlyn, B. E., Messier, J., Moles, A. T., Müller, S. C., Nadrowski, K., Naeem, S., Niinemets, Ü., Nöllert, S., Nüske, A., Ogaya, R., Oleksyn, J., Onipchenko, V. G., Onoda, Y., Ordoñez, J., Overbeck, G., Ozinga, W. A., Patiño, S., Paula, S., Pausas, J. G., Peñuelas, J., Phillips, O. L., Pillar, V., Poorter, H., Poorter, L., Poschlod, P., Prinzing, A., Proulx, R., Rammig, A., Reinsch, S., Reu, B., Sack, L., Salgado-Negret, B., Sardans, J.,



- 895 Shiodera, S., Shipley, B., Siefert, A., Sosinski, E., Soussana, J.-F., Swaine, E., Swenson, N., Thompson, K., Thornton, P.,
Waldram, M., Weiher, E., White, M., White, S., Wright, S. J., Yguel, B., Zaehle, S., Zanne, A. E., and Wirth, C.: TRY - a
global database of plant traits, *Glob. Chang. Biol.*, 17, 2905–2935, <https://doi.org/10.1111/j.1365-2486.2011.02451.x>,
2011.
- 900 Kautz, M., Meddens, A. J. H., Hall, R. J., and Arneeth, A.: Biotic disturbances in Northern Hemisphere forests – a synthesis of
recent data, uncertainties and implications for forest monitoring and modelling, *Glob. Ecol. Biogeogr.*, 26(5), 533–552,
<https://doi.org/10.1111/geb.12558>, 2017.
- Kautz, M., Arneeth, A., Anthoni, P., Meddens, A. J. H., Pugh, T. A. M., and Arneeth, A.: Simulating the recent impacts of
multiple biotic disturbances on forest carbon cycling across the United States, *Glob. Chang. Biol.*, 24, 2079–2092,
<https://doi.org/10.1111/gcb.13974>, 2018.
- 905 Kennedy, D., Swenson, S., Oleson, K. W., Lawrence, D. M., Fisher, R., Lola da Costa, A. C., and Gentine, P.: Implementing
plant hydraulics in the Community Land Model, Version 5, *J. Adv. Model. Earth Syst.*, 11, 485–513,
<https://doi.org/10.1029/2018MS001500>, 2019.
- Krinner, G., Viovy, N., de Noblet-Ducoudré, N., Ogée, J., Polcher, J., Friedlingstein, P., Ciais, P., Sitch, S., and Prentice, I.
C.: A dynamic global vegetation model for studies of the coupled atmosphere-biosphere system, *Global Biogeochem.
Cycles*, 19, GB1015, <https://doi.org/10.1029/2003GB002199>, 2005.
- 910 Lamarque, J.-F., Dentener, F., McConnell, J., Ro, C. U., Shaw, M., Vet, R., Bergmann, D., Cameron-Smith, P., Dalsoren, S.,
Doherty, R., Faluvegi, G., Ghan, S. J., Josse, B., Lee, Y. H., MacKenzie, I. A., Plummer, D., Shindell, D. T., Skeie, R. B.,
Stevenson, D. S., Strode, S., Zeng, G., Curran, M., Dahl-Jensen, D., Das, S., Fritzsche, D., and Nolan, M.: Multi-model
mean nitrogen and sulfur deposition from the atmospheric chemistry and climate model intercomparison project
(ACCMIP): Evaluation of historical and projected future changes, *Atmos. Chem. Phys.*, 13(16), 7997–8018,
915 <https://doi.org/10.5194/acp-13-7997-2013>, 2013.
- Landry, J. S., Price, D. T., Ramankutty, N., Parrott, L., and Damon Matthews, H.: Implementation of a Marauding Insect
Module (MIM, version 1.0) in the Integrated Biosphere Simulator (IBIS, version 2.6b4) dynamic vegetation-land surface
model, *Geosci. Model Dev.*, 9(3), 1243–1261, <https://doi.org/10.5194/gmd-9-1243-2016>, 2016.
- 920 Langan, L., Higgins, S. I., and Scheiter, S.: Climate-biomes, pedo-biomes or pyro-biomes: which world view explains the
tropical forest-savanna boundary in South America?, *J. Biogeogr.*, 44, 2319–2330, <https://doi.org/10.1111/jbi.13018>, 2017.
- Lehsten, V., Mischurrow, M., Lindström, E., Lehsten, D., and Lischke, H.: LPJ-GM 1.0: simulating migration efficiently in a
dynamic vegetation model, *Geosci. Model Dev.*, 12, 893–908, <https://doi.org/10.5194/gmd-12-893-2019>, 2019.
- 925 Le Quéré, C., Moriarty, R., Andrew, R. M., Canadell, J. G., Sitch, S., Korsbakken, J. I., Friedlingstein, P., Peters, G. P.,
Andres, R. J., Boden, T. A., Houghton, R. A., House, J. I., Keeling, R. F., Tans, P., Arneeth, A., Bakker, D. C. E., Barbero,
L., Bopp, L., Chang, J., Chevallier, F., Chini, L. P., Ciais, P., Fader, M., Feely, R. A., Gkritzalis, T., Harris, I., Hauck, J.,
Ilyina, T., Jain, A. K., Kato, E., Kitidis, V., Klein Goldewijk, K., Koven, C., Landschützer, P., Lauvset, S. K., Lefèvre, N.,
Lenton, A., Lima, I. D., Metzl, N., Millero, F., Munro, D. R., Murata, A., Nabel, J. E. M. S., Nakaoka, S., Nojiri, Y.,
O'Brien, K., Olsen, A., Ono, T., Pérez, F. F., Pfeil, B., Pierrot, D., Poulter, B., Rehder, G., Rödenbeck, C., Saito, S.,
Schuster, U., Schwinger, J., Séférian, R., Steinhoff, T., Stocker, B. D., Sutton, A. J., Takahashi, T., Tilbrook, B., van der
930 Laan-Luijkx, I. T., van der Werf, G. R., van Heuven, S., Vandemark, D., Viovy, N., Wiltshire, A., Zaehle, S., and Zeng,
N.: Global Carbon Budget 2015, *Earth Syst. Sci. Data*, 7, 349–396, <https://doi.org/10.5194/essd-7-349-2015>, 2015.
- Le Quéré, C., Andrew, R. M., Friedlingstein, P., Sitch, S., Pongratz, J., Manning, A. C., Korsbakken, J. I., Peters, G. P.,
Canadell, J. G., Jackson, R. B., Boden, T. A., Tans, P. P., Andrews, O. D., Arora, V. K., Bakker, D. C. E., Barbero, L.,
935 Becker, M., Betts, R. A., Bopp, L., Chevallier, F., Chini, L. P., Ciais, P., Cosca, C. E., Cross, J., Currie, K., Gasser, T.,
Harris, I., Hauck, J., Haverd, V., Houghton, R. A., Hunt, C. W., Hurtt, G., Ilyina, T., Jain, A. K., Kato, E., Kautz, M.,
Keeling, R. F., Klein Goldewijk, K., Körtzinger, A., Landschützer, P., Lefèvre, N., Lenton, A., Lienert, S., Lima, I.,
Lombardozzi, D., Metzl, N., Millero, F., Monteiro, P. M. S., Munro, D. R., Nabel, J. E. M. S., Nakaoka, S., Nojiri, Y.,
Padin, X. A., Peregon, A., Pfeil, B., Pierrot, D., Poulter, B., Rehder, G., Reimer, J., Rödenbeck, C., Schwinger, J., Séférian,
R., Skjelvan, I., Stocker, B. D., Tian, H., Tilbrook, B., Tubiello, F. N., van der Laan-Luijkx, I. T., van der Werf, G. R., van
940 Heuven, S., Viovy, N., Vuichard, N., Walker, A. P., Watson, A. J., Wiltshire, A. J., Zaehle, S., and Zhu, D.: Global Carbon
Budget 2017, *Earth Syst. Sci. Data*, 10(1), 405–448, <https://doi.org/10.5194/essd-10-405-2018>, 2018.
- Liang, J., Crowther, T. W., Picard, N., Wiser, S., Zhou, M., Alberti, G., Schulze, E.-D., McGuire, A. D., Bozzato, F., Pretzsch,
H., de-Miguel, S., Paquette, A., Hérault, B., Scherer-Lorenzen, M., Barrett, C. B., Glick, H. B., Hengeveld, G. M., Nabuurs,



- 945 G.-J., Pfautsch, S., Viana, H., Vibrans, A. C., Ammer, C., Schall, P., Verbyla, D., Tchebakova, N., Fischer, M., Watson, J. V., Chen, H. Y. H., Lei, X., Schelhaas, M.-J., Lu, H., Gianelle, D., Parfenova, E. I., Salas, C., Lee, E., Lee, B., Kim, H. S., Bruelheide, H., Coomes, D. A., Piotta, D., Sunderland, T., Schmid, B., Gourlet-Fleury, S., Sonké, B., Tavani, R., Zhu, J., Brandl, S., Vayreda, J., Kitahara, F., Searle, E.B., Neldner, V.J., Ngugi, M.R., Baraloto, C., Frizzera, L., Balazy, R., Oleksyn, J., Zawila-Niedzwiecki, T., Bouriaud, O., Bussotti, F., Finér, L., Jaroszewicz, B., Jucker, T., Valladares, F., Jagodzinski, A.M., Peri, P. L., Gonmadje, C., Marthy, W., O'Brien, T., Martin, E. H., Marshall, A. R., Rovero, F., Bitariho, R., Niklaus, P. A., Alvarez-Loayza, P., Chamuya, N., Valencia, R., Mortier, F., Wortel, V., Engone-Obiang, N. L., Ferreira, L. V., Odeke, D. E., Vasquez, R. M., Lewis, S. L., and Reich, P. B.: Positive biodiversity-productivity relationship predominant in global forests, *Science*, 354(6309), aaf8957, <https://doi.org/10.1126/science.aaf8957>, 2016.
- 950 Lines, E. R., Coomes, D. A., and Purves, D. W.: Influences of forest structure, climate and species composition on tree mortality across the Eastern US, *PLoS One*, 5(10), e13212, <https://doi.org/10.1371/journal.pone.0013212>, 2010.
- 955 Liu, Y., Parolari, A. J., Kumar, M., Huang, C.-W., Katul, G. G., and Porporato, A.: Increasing atmospheric humidity and CO₂ concentration alleviate forest mortality risk, *Proc. Natl. Acad. Sci.*, 201704811, <https://doi.org/10.1073/pnas.1704811114>, 2017.
- Lukac, M.: Fine root turnover, in: *Measuring Roots: An Updated Approach*, in *Fine Root Turnover*, edited by S. Mancuso, pp. 363–373, Springer, Heidelberg, <https://doi.org/10.1007/978-3-642-22067-8>, 2012.
- 960 Marvin, D. C. and Asner, G. P.: Branchfall dominates annual carbon flux across lowland Amazonian forests, *Environ. Res. Lett.*, 11, 094027, 2016.
- Matamala, R., González-Meler, M. A., Jastrow, J. D., Norby, R. J., and Schlesinger, W. H.: Impacts of fine root turnover on forest NPP and soil C sequestration potential, *Science*, 302, 1385–1387, <https://doi.org/10.1126/science.1089543>, 2003.
- 965 McDowell, N., Pockman, W. T., Allen, C. D., Breshears, D. D., Cobb, N., Kolb, T., Plaut, J., Sperry, J., West, A., Williams, D. G., and Yezzer, E. A.: Mechanisms of plant survival and mortality during drought: why do some plants survive while others succumb to drought?, *New Phytol.*, 178(4), 719–739, <https://doi.org/10.1111/j.1469-8137.2008.02436.x>, 2008.
- McDowell, N., Allen, C. D., Anderson-Teixeira, K., Brando, P., Brienen, R., Chambers, J., Christoffersen, B., Davies, S., Doughty, C., Duque, A., Espirito-Santo, F., Fisher, R., Fontes, C. G., Galbraith, D., Goodsman, D., Grossiord, C., Hartmann, H., Holm, J., Johnson, D. J., Kassim, A. R., Keller, M., Koven, C., Kueppers, L., Kumagai, T., Malhi, Y., 970 McMahon, S. M., Mencuccini, M., Meir, P., Moorcroft, P., Muller-Landau, H. C., Phillips, O. L., Powell, T., Sierra, C. A., Sperry, J., Warren, J., Xu, C., and Xu, X.: Drivers and mechanisms of tree mortality in moist tropical forests, *New Phytol.*, 219(3), 851–869, <https://doi.org/10.1111/nph.15027>, 2018.
- McDowell, N. G.: Mechanisms linking drought, hydraulics, carbon metabolism, and vegetation mortality., *Plant Physiol.*, 155(3), 1051–1059, <https://doi.org/10.1104/pp.110.170704>, 2011.
- 975 McDowell, N. G., Beerling, D. J., Breshears, D. D., Fisher, R. A., Raffa, K. F., and Stitt, M.: The interdependence of mechanisms underlying climate-driven vegetation mortality, *Trends Ecol. Evol.*, 26(10), 523–532, <https://doi.org/10.1016/j.tree.2011.06.003>, 2011.
- McDowell, N. G., Coops, N. C., Beck, P. S. A., Chambers, J. Q., Gangodagamage, C., Hicke, J. A., Huang, C., Kennedy, R., Krofcheck, D. J., Litvak, M., Meddens, A. J. H., Muss, J., Negrón-Juarez, R., Peng, C., Schwantes, A. M., Swenson, J. J., 980 Vernon, L. J., Williams, A. P., Xu, C., Zhao, M., Running, S. W., and Allen, C. D.: Global satellite monitoring of climate-induced vegetation disturbances, *Trends Plant Sci.*, 20(2), 114–123, <https://doi.org/10.1016/j.tplants.2014.10.008>, 2015.
- McGrath, M. J., Luyssaert, S., Meyfroidt, P., Kaplan, J. O., Bürgi, M., Chen, Y., Erb, K., Gimmi, U., McInerney, D., Naudts, K., Otto, J., Pasztor, F., Ryder, J., Schelhaas, M.-J., and Valade, A.: Reconstructing European forest management from 1600 to 2010, *Biogeosciences*, 12, 4291–4316, <https://doi.org/10.5194/bg-12-4291-2015>, 2015.
- 985 Medlyn, B. E., Zaehle, S., De Kauwe, M. G., Walker, A. P., Dietze, M. C., Hanson, P. J., Hickler, T., Jain, A. K., Luo, Y., Parton, W., Prentice, I. C., Thornton, P. E., Wang, S., Wang, Y.-P., Weng, E., Iversen, C. M., McCarthy, H. R., Warren, J. M., Oren, R., and Norby, R. J.: Using ecosystem experiments to improve vegetation models, *Nat. Clim. Chang.*, 5(6), 528–534, <https://doi.org/10.1038/nclimate2621>, 2015.
- 990 Meier, E. S., Lischke, H., Schmatz, D. R., and Zimmermann, N. E.: Climate, competition and connectivity affect future migration and ranges of European trees, *Glob. Ecol. Biogeogr.*, 21, 164–178, doi:10.1111/j.1466-8238.2011.00669.x, 2012.
- Muscolo, A., Bagnato, S., Sidari, M., and Mercurio, R.: A review of the roles of forest canopy gaps, *J. For. Res.*, 25(4), 725–736, <https://doi.org/10.1007/s11676-014-0521-7>, 2014.



- 995 Negrón-Juárez, R. I., Holm, J. A., Marra, D. M., Rifai, S. W., Riley, W. J., Chambers, J. Q., Koven, C. D., Knox, R. G.,
McGroddy, M. E., Di Vittorio, A. V., Urquiza-Muñoz, J., Tello-Espinoza, R., Muñoz, W. A., Ribeiro, G. H. P. M., and
Higuchi, N.: Vulnerability of Amazon forests to storm-driven tree mortality, *Environ. Res. Lett.*, 13(5),
<https://doi.org/10.1088/1748-9326/aabe9f>, 2018.
- 000 Nishina, K., Ito, A., Falloon, P., Friend, A. D., Beerling, D. J., Ciais, P., Clark, D. B., Kahana, R., Kato, E., Lucht, W., Lomas,
M., Pavlick, R., Schaphoff, S., Warszawski, L., and Yokohata, T.: Decomposing uncertainties in the future terrestrial
carbon budget associated with emission scenarios, climate projections, and ecosystem simulations using the ISI-MIP
results, *Earth Syst. Dyn.*, 6(2), 435–445, <https://doi.org/10.5194/esd-6-435-2015>, 2015.
- 005 Norby, R. J., De Kauwe, M. G., Domingues, T. F., Duursma, R. A., Ellsworth, D. S., Goll, D. S., Lapola, D. M., Luus, K. A.,
MacKenzie, A. R., Medlyn, B. E., Pavlick, R., Rammig, A., Smith, B., Thomas, R., Thonicke, K., Walker, A. P., Yang,
X., and Zaehle, S.: Model-data synthesis for the next generation of forest free-air CO₂ enrichment (FACE) experiments,
New Phytol., 209, 17–28, <https://doi.org/10.1111/nph.13593>, 2016.
- Parazoo, N. C., Arneeth, A., Pugh, T. A. M., Smith, B., Steiner, N., Luus, K., Commane, R., Benmergui, J., Stofferahn, E., Liu,
J., Rödenbeck, C., Kawa, R., Euskirchen, E., Zona, D., Arndt, K., Oechel, W., and Miller, C.: Spring photosynthetic onset
and net CO₂ uptake in Alaska triggered by landscape thawing, *Glob. Chang. Biol.*, 24(8), 3416–3435,
<https://doi.org/10.1111/gcb.14283>, 2018.
- 010 Pavlick, R., Drewry, D. T., Bohn, K., Reu, B., and Kleidon, A.: The Jena Diversity-Dynamic Global Vegetation Model (JeDi-
DGVM): a diverse approach to representing terrestrial biogeography and biogeochemistry based on plant functional trade-
offs, *Biogeosciences*, 10, 4137–4177, <https://doi.org/10.5194/bg-10-4137-2013>, 2013.
- Peng, C., Ma, Z., Lei, X., Zhu, Q., Chen, H., Wang, W., Liu, S., Li, W., Fang, X., and Zhou, X.: A drought-induced pervasive
increase in tree mortality across Canada's boreal forests, *Nat. Clim. Chang.*, 1(12), 467–471,
015 <https://doi.org/10.1038/nclimate1293>, 2011.
- Phillips, O. L., van der Heijden, G., Lewis, S. L., López-González, G., Aragão, L.E., Lloyd, J., Malhi, Y., Monteagudo, A.,
Almeida, S., Dávila, E. A., Amaral, I., Andelman, S., Andrade, A., Arroyo, L., Aymard, G., Baker, T. R., Blanc, L., Bonal,
D., de Oliveira, A.C., Chao, K.J., Cardozo, N.D., da Costa, L., Feldpausch, T. R., Fisher, J. B., Fyllas, N. M., Freitas, M.
A., Galbraith, D., Gloor, E., Higuchi, N., Honorio, E., Jimeénez, E., Keeling, H., Killeen, T. J., Gloor, E., Higuchi, N.,
020 Lovett, J. C., Meir, P., Mendoza, C., Morel, A., Nuñez Vargas, P. N., Patiño, S., Peh, K.S., Cruz, A.P., Prieto, A., Quesada,
C. A., Peh, K. S., Peña Cruz, A., Prieto, A., Quesada, C. A., Ramirez, F., Ramirez, H., Rudas, A., Salamã, R., Schwarz,
M., Silva, J., Silveira, M., Slik, J. W. F., Sonké, B., Sota Thomas, A., Stropp, J., Taplin, J. R. D., Vásquez, R., and Vilanova,
E.: Drought-mortality relationships for tropical forests, *New Phytol.*, 187, 631–646, <https://doi.org/10.1111/j.1469-8137.2010.03359.x>, 2010.
- 025 Pillet, M., Joetzer, E., Belmin, C., Chave, J., Ciais, P., Dourdain, A., Evans, M., Hérault, B., Luysaert, S., Poulter, B., and
Poulter, B.: Disentangling competitive vs. climatic drivers of tropical forest mortality, *J. Ecol.*, 106, 1165–1179,
<https://doi.org/10.1111/1365-2745.12876>, 2018.
- Poorter, L., Rozendaal, D. M. A., Bongers, F., de Almeida-Cortez, J. S., Almeyda Zambrano, A. M., Álvarez, F. S., Andrade,
J. L., Villa, L. F. A., Balvanera, P., Becknell, J. M., Bentos, T. V., Bhaskar, R., Boukili, V., Brancalion, P. H. S., Broadbent,
030 E. N., César, R. G., Chave, J., Chazdon, R. L., Colletta, G. D., Craven, D., de Jong, B. H. J., Denslow, J. S., Dent, D. H.,
DeWalt, S. J., García, E. D., Dupuy, J. M., Durán, S. M., Espírito Santo, M. M., Fandiño, M. C., Fernandes, G. W., Finegan,
B., Moser, V. G., Hall, J. S., Hernández-Stefanoni, J. L., Jakovac, C. C., Junqueira, A. B., Kennard, D., Lebrija-Trejos, E.,
Letcher, S. G., Lohbeck, M., Lopez, O. R., Marín-Spiotta, E., Martínez-Ramos, M., Martins, S. V., Massoca, P. E. S.,
Meave, J. A., Mesquita, R., Mora, F., de Souza Moreno, V., Müller, S. C., Muñoz, R., Muscarella, R., de Oliveira Neto, S.
035 N., Nunes, Y. R. F., Ochoa-Gaona, S., Paz, H., Peña-Claros, M., Piotta, D., Ruíz, J., Sanaphre-Villanueva, L., Sanchez-
Azofeifa, A., Schwartz, N. B., Steininger, M. K., Thomas, W. W., Toledo, M., Uriarte, M., Utrera, L. P., van Breugel, M.,
van der Sande, M. T., van der Wal, H., Veloso, M. D. M., Vester, H. F. M., Vieira, I. C. G., Villa, P. M., Williamson, G.
B., Wright, S. J., Zanini, K. J., Zimmerman, J. K., and Westoby, M.: Wet and dry tropical forests show opposite
040 successional pathways in wood density but converge over time, *Nat. Ecol. Evol.*, 3(6), 928–934,
<https://doi.org/10.1038/s41559-019-0882-6>, 2019.
- Poulter, B., MacBean, N., Hartley, A., Khlystova, I., Arino, O., Betts, R., Bontemps, S., Boettcher, M., Brockmann, C.,
Defourny, P., Hagemann, S., Herold, M., Kirches, G., Lamarche, C., Lederer, D., Ottlé, C., Peters, M., and Peylin, P.: Plant
functional type classification for earth system models: results from the European Space Agency's Land Cover Climate



- Change Initiative, *Geosci. Model Dev.*, 8, 2315–2328, <https://doi.org/10.5194/gmd-8-2315-2015>, 2015.
- 045 Pretzsch, H.: Species-specific allometric scaling under self-thinning: evidence from long-term plots in forest stands, *Oecologia*, 146, 572–583, <https://doi.org/10.1007/s00442-005-0126-0>, 2006.
- Pretzsch, H., Biber, P., Schütze, G., Uhl, E., and Rötzer, T.: Forest stand growth dynamics in Central Europe have accelerated since 1870, *Nat. Commun.*, 5, 4967, <https://doi.org/10.1038/ncomms5967>, 2014.
- 050 Pugh, T. A. M., Müller, C., Arneth, A., Haverd, V., and Smith, B.: Key knowledge and data gaps in modelling the influence of CO₂ concentration on the terrestrial carbon sink, *J. Plant Physiol.*, 203, 3–15, <https://doi.org/10.1016/j.jplph.2016.05.001>, 2016.
- Pugh, T. A. M., Arneth, A., Kautz, M., Poulter, B., and Smith, B.: Important role of forest disturbances in the global biomass turnover and carbon sinks, *Nat. Geosci.*, 12, 730–735, <https://doi.org/10.1038/s41561-019-0427-2>, 2019a.
- Pugh, T. A. M., Lindeskog, M., Smith, B., Poulter, B., Arneth, A., Haverd, V., and Calle, L.: The role of forest regrowth in global carbon sink dynamics, *Proc. Natl. Acad. Sci. U. S. A.*, 116(10), 4382–4387, <https://doi.org/10.1073/pnas.1810512116>, 2019b.
- 055 Reich, P. B.: The world-wide ‘fast-slow’ plant economics spectrum: a traits manifesto, *J. Ecol.*, 102, 275–301, <https://doi.org/10.1111/1365-2745.12211>, 2014.
- Reich, P. B., Walters, M. B., and Ellsworth, D. S.: From tropics to tundra: Global convergence in plant functioning, *Proc. Natl. Acad. Sci. U. S. A.*, 94, 13730–13734, <https://doi.org/10.1073/pnas.94.25.13730>, 1997.
- 060 Rowland, L., da Costa, A. C. L., Galbraith, D. R., Oliveira, R. S., Binks, O. J., Oliveira, A. A. R., Pullen, A. M., Doughty, C. E., Metcalfe, D. B., Vasconcelos, S. S., Ferreira, L. V., Malhi, Y., Grace, J., Mencuccini, M., and Meir, P.: Death from drought in tropical forests is triggered by hydraulics not carbon starvation., *Nature*, 528(7580), 119–122, <https://doi.org/10.1038/nature15539>, 2015.
- 065 Ruiz-Benito, P., Ratcliffe, S., Jump, A. S., Gómez-Aparicio, L., Madrigal-González, J., Wirth, C., Kändler, G., Lehtonen, A., Dahlgren, J., Kattge, J., and Zavala, M. A.: Functional diversity underlies demographic responses to environmental variation in European forests, *Glob. Ecol. Biogeogr.*, 26, 128–141, <https://doi.org/10.1111/geb.12515>, 2016.
- Ryan, M. G., Phillips, N., and Bond, B. J.: The hydraulic limitation hypothesis revisited, *Plant, Cell Environ.*, 29(3), 367–381, <https://doi.org/10.1111/j.1365-3040.2005.01478.x>, 2006.
- 070 Saatchi, S. S., Harris, N. L., Brown, S., Lefsky, M., Mitchard, E. T. A., Salas, W., Zutta, B. R., Buermann, W., Lewis, S. L., Hagen, S., Petrova, S., White, L., Silman, M., and Morel, A.: Benchmark map of forest carbon stocks in tropical regions across three continents, *Proc. Natl. Acad. Sci.*, 108, 9899–9904, <https://doi.org/10.1073/pnas.1019576108>, 2011.
- Sakschewski, B., von Bloh, W., Boit, A., Rammig, A., Kattge, J., Poorter, L., Peñuelas, J., and Thonicke, K.: Leaf and stem economics spectra drive diversity of functional plant traits in a dynamic global vegetation model, *Glob. Chang. Biol.*, 21, 2711–2725, <https://doi.org/10.1111/gcb.12870>, 2015.
- 075 Salguero-Gómez, R., Jones, O. R., Jongejans, E., Blomberg, S. P., Hodgson, D. J., Mbeau-Ache, C., Zuidema, P.A., de Kroon, H., and Buckley, Y.M.: Fast – slow continuum and reproductive strategies structure plant life-history variation worldwide, *Proc. Natl. Acad. Sci. U. S. A.*, 113(1), 230–235, <https://doi.org/10.1073/pnas.1506215112>, 2016.
- Sato, H., Itoh, A., and Kohyama, T.: SEIB-DGVM: A new Dynamic Global Vegetation Model using a spatially explicit individual-based approach, *Ecol. Modell.*, 200, 279–307, <https://doi.org/10.1016/j.ecolmodel.2006.09.006>, 2007.
- 080 Schaphoff, S., Lucht, W., Gerten, D., Sitch, S., Cramer, W., and Prentice, I. C.: Terrestrial biosphere carbon storage under alternative climate projections, *Clim. Change*, 74(1–3), 97–122, <https://doi.org/10.1007/s10584-005-9002-5>, 2006.
- Schaphoff, S., Forkel, M., Müller, C., Knauer, J., von Bloh, W., Gerten, D., Jägermeyr, J., Lucht, W., Rammig, A., Thonicke, K., and Waha, K.: LPJmL4 – a dynamic global vegetation model with managed land – Part 2: Model evaluation, *Geosci. Model Dev.*, 11, 1377–1403, <https://doi.org/10.5194/gmd-11-1377-2018>, 2018.
- 085 Scheiter, S., Langan, L., and Higgins, S. I.: Next-generation dynamic global vegetation models: learning from community ecology, *New Phytol.*, 198(3), 957–969, <https://doi.org/10.1111/nph.12210>, 2013.
- Schelhaas, M.-J., Fridman, J., Hengeveld, G. M., Henttonen, H. M., Lehtonen, A., Kies, U., Krajnc, N., Lerink, B., Dhubháin, A. N., Polley, H., Pugh, T. A. M., Redmond, J. J., Rohner, B., Temperli, C., Vayreda, J., and Nabuurs, G.-J.: Actual European forest management by region, tree species and owner based on 714,000 re-measured trees in national forest inventories, *PLoS One*, 13(11), e0207151, 2018.
- 090 Schumacher, S., Reineking, B., Sibold, J., and Bugmann, H.: Modeling the impact of climate and vegetation on fire regimes in mountain landscapes, *Landsc. Ecol.*, 21, 539–554, <https://doi.org/10.1007/s10980-005-2165-7>, 2006.



- 095 Seidl, R., Schelhaas, M.-J., Rammer, W., and Verkerk, P. J.: Increasing forest disturbances in Europe and their impact on carbon storage, *Nat. Clim. Chang.*, 4, 806–810, <https://doi.org/10.1038/nclimate2318>, 2014.
- Seidl, R., Thom, D., Kautz, M., Martin-Benito, D., Peltoniemi, M., Vacchiano, G., Wild, J., Ascoli, D., Petr, M., Honkaniemi, J., Lexer, M. J., Trotsuik, V., Mairota, P., Svobody, M., Fabrika, M., Nagel, T. A., and Reyer, C. P. O.: Forest disturbances under climate change, *Nat. Clim. Chang.*, 7(6), 395–402, <https://doi.org/10.1038/nclimate3303>, 2017.
- 100 Sevanto, S., McDowell, N. G., Dickman, L. T., Pangle, R., and Pockman, W. T.: How do trees die? A test of the hydraulic failure and carbon starvation hypotheses., *Plant. Cell Environ.*, 37(1), 153–161, <https://doi.org/10.1111/pce.12141>, 2014.
- Sierra, C. A., Müller, M., Metzler, H., Manzoni, S., and Trumbore, S. E.: The muddle of ages, turnover, transit, and residence times in the carbon cycle, *Glob. Chang. Biol.*, 23(5), 1763–1773, <https://doi.org/10.1111/gcb.13556>, 2017.
- 105 Sitch, S., Smith, B., Prentice, I. C., Arneth, A., Bondeau, A., Cramer, W., Kaplan, J. O., Levis, S., Lucht, W., Sykes, M. T., Thonicke, K., and Venevsky, S.: Evaluation of ecosystem dynamics, plant geography and terrestrial carbon cycling in the LPJ dynamic global vegetation model, *Glob. Chang. Biol.*, 9, 161–185, <https://doi.org/10.1046/j.1365-2486.2003.00569.x>, 2003.
- Sitch, S., Huntingford, C., Gedney, N., Levy, P. E., Lomas, M., Piao, S. L., Betts, R., Ciais, P., Cox, P., Friedlingstein, P., Jones, C. D., Prentice, I. C., and Woodward, F. I.: Evaluation of the terrestrial carbon cycle, future plant geography and climate-carbon cycle feedbacks using five Dynamic Global Vegetation Models (DGVMs), *Glob. Chang. Biol.*, 14, 2015–2039, <https://doi.org/10.1111/j.1365-2486.2008.01626.x>, 2008.
- 110 Smith, B., Wärlind, D., Arneth, A., Hickler, T., Leadley, P., Siltberg, J., and Zaehle, S.: Implications of incorporating N cycling and N limitations on primary production in an individual-based dynamic vegetation model, *Biogeosciences*, 11(7), 2027–2054, <https://doi.org/10.5194/bg-11-2027-2014>, 2014.
- Steinkamp, J. and Hickler, T.: Is drought-induced forest dieback globally increasing?, *J. Ecol.*, 103, 31–43, <https://doi.org/10.1111/1365-2745.12335>, 2015.
- 115 Thonicke, K., Venevsky, S., Sitch, S., and Cramer, W.: The role of fire disturbance for global vegetation dynamics: coupling fire into a Dynamic Global Vegetation Model, *Glob. Ecol. Biogeogr.*, 10(6), 661–677, <https://doi.org/10.1046/j.1466-822X.2001.00175.x>, 2001.
- Thurner, M., Beer, C., Santoro, M., Carvalhais, N., Wutzler, T., Schepaschenko, D., Shvidenko, A., Kompter, E., Ahrens, B., 120 Levick, S. R., and Schmullius, C.: Carbon stocks and density of northern boreal and temperate forests, *Glob. Ecol. Biogeogr.*, 23, 297–310, <https://doi.org/10.1111/geb.12125>, 2014.
- Thurner, M., Beer, C., Ciais, P., Friend, A. D., Ito, A., Kleidon, A., Lomas, M. R., Quegan, S., Rademacher, T. T., Schaphoff, S., Tum, M., Wiltshire, A., and Carvalhais, N.: Evaluation of climate-related carbon turnover processes in global vegetation models for boreal and temperate forests, *Glob. Chang. Biol.*, 23, 3076–3091, <https://doi.org/10.1111/gcb.13660>, 2017.
- 125 Tomlinson, K. W., Sterck, F. J., Bongers, F., da Silva, D. A., Barbosa, E. R. M., Ward, D., Bakker, F. T., van Kaauwen, M., Prins, H. H. T., de Bie, S., and van Langevelde, F.: Biomass partitioning and root morphology of savanna trees across a water gradient, *J. Ecol.*, 100, 1113–1121, <https://doi.org/10.1111/j.1365-2745.2012.01975.x>, 2012.
- Tum, M., Zeidler, J. N., Günther, K. P., and Esch, T.: Global NPP and straw bioenergy trends for 2000–2014, *Biomass and Bioenergy*, 90, 230–236, <https://doi.org/10.1016/j.biombioe.2016.03.040>, 2016.
- 130 Van Mantgem, P. J., Stephenson, N. L., Byrne, J. C., Daniels, L. D., Franklin, J. F., Fulé, P. Z., Harmon, M. E., Larson, A. J., Smith, J. M., Taylor, A. H., and Veblen, T. T.: Widespread increase of tree mortality rates in the western United States., *Science*, 323(January), 521–524, <https://doi.org/10.1126/science.1165000>, 2009.
- Walker, A. P., De Kauwe, M. G., Medlyn, B. E., Zaehle, S., Iverson, C. M., Asao, S., Guenet, B., Harper, A., Hickler, T., Hungate, B. A., Jain, A. K., Luo, Y., Lu, X., Lu, M., Luus, K., Megonigal, J. P., Oren, R., Ryna, E., Shu, S., Talhelm, A., 135 Wang, Y.-P., Warren, J. M., Werner, C., Xia, J., Yang, B., Zak, D. R., and Norby, R. J.: Decadal biomass increment in early secondary succession woody ecosystems is increased by CO₂ enrichment, *Nat. Commun.*, 10, 454, <https://doi.org/10.1038/s41467-019-08348-1>, 2019.
- Wenk, E. H. and Falster, D. S.: Quantifying and understanding reproductive allocation schedules in plants, *Ecol. Evol.*, 5(23), 5521–5538, <https://doi.org/10.1002/ece3.1802>, 2015.
- 140 Westoby, M.: The self-thinning rule, *Adv. Ecol. Res.*, 14, 167–225, doi:10.1016/S0065-2504(08)60171-3, 1984.
- Wißkirchen, K., Tum, M., Günther, K. P., Niklaus, M., Eisfelder, C., and Knorr, W.: Quantifying the carbon uptake by vegetation for Europe on a 1 km² resolution using a remote sensing driven vegetation model, *Geosci. Model Dev.*, 6, 1623–1640, <https://doi.org/10.5194/gmd-6-1623-2013>, 2013.



- 145 Würth, M. K. R., Winter, K., and Körner, C. H.: In situ responses to elevated CO₂ in tropical forest understorey plants, *Funct. Ecol.*, 12, 886–895, <https://doi.org/10.1046/j.1365-2435.1998.00278.x>, 1998.
- Xu, X., Medvigy, D., Powers, J. S., Becknell, J. M., and Guan, K.: Diversity in plant hydraulic traits explains seasonal and inter-annual variations of vegetation dynamics in seasonally dry tropical forests, *New Phytol.*, 212, 80–95, <https://doi.org/10.1111/nph.14009>, 2016.
- 150 Yuan, Z. Y. and Chen, H. Y. H.: Fine root biomass, production, turnover rates, and nutrient contents in boreal forest ecosystems in relation to species, climate, fertility, and stand age: Literature review and meta-analyses, *CRC. Crit. Rev. Plant Sci.*, 29(4), 204–221, <https://doi.org/10.1080/07352689.2010.483579>, 2010.
- Zhao, M. and Running, S. W.: Drought-induced reduction in global terrestrial net primary production from 2000 through 2009, *Science*, 329, 940–943, <https://doi.org/10.1126/science.1192666>, 2010.
- 155 Zhu, K., Woodall, C. W., and Clark, J. S.: Failure to migrate: lack of tree range expansion in response to climate change, *Glob. Chang. Biol.*, 18, 1042–1052, <https://doi.org/10.1111/j.1365-2486.2011.02571.x>, 2012.



160
 165

Table 1. Conceptualisation of mechanisms by which biomass stock or τ can be modified as a result of environmental change. Mechanisms are grouped by those related to the existing functional composition of trees and those related to a change of tree functional composition. The change in biomass and τ due to a change in resource allocation, mortality turnover rate or phenological turnover rate is illustrated. A dash indicates no change. The change for each mechanism is conceptualised in a particular direction, consistent with the given example, but could equally apply in reverse. For instance, MI_{MR} could also be shown with a decreased mortality rate, leading to increased biomass and τ . The groupings correspond to those commonly used in TBMs, with “mortality” referring to turnover from wood resulting from tree death, and “phenological” referring to turnover of “soft” tissues, which include leaves, fine roots and fruits. For simplicity, rapidly turned-over components such as root exudates and biogenic volatile organic compound emissions, which are rarely explicitly represented in TBMs, are lumped into the categories “soft” and “phenological” for allocation and turnover, respectively, although it is noted that some TBM parameterisations may implicitly include the lost carbon in respiration fluxes. Codes (e.g. MI_{MR}) are introduced and used in the main text to refer to the individual mechanisms.

	Resource capture (NPP) and allocation to woody or soft tissue	Mortality turnover rate	Phenological turnover rate	Biomass	τ	Example driver
PFT-level response (i.e. functional composition unchanged)						
MI_{MR} . Changed mortality rate						More severe drought, demographic shift
$MI_{NPP,F}$. Changed NPP, fixed allocation frac.						CO ₂ fertilisation
$MI_{NPP,FS}$. Changed NPP, fixed soft allocation						CO ₂ fertilisation
MI_{RA} . Shifted resource allocation						Water/Nutrient shortage (more roots)
MI_{ST} . Changed soft turnover rate						Water/Nutrient shortage (more exudates)
Stand-level response (with functional composition unchanged)						
MS_{comp} . Changed NPP, changed competition						CO ₂ fertilisation accelerates self-thinning
Population-level response (due to shift in functional composition of species)						
MP_{MR} . Different mortality rate						Reduced defensive investment
MP_{NPP} . Different intrinsic NPP						More conservative strategy
MP_{RA} . Different carbon allocation						Reduced wood density
MP_{ST} . Different soft turnover rate						Shift in phenology / exudate prod.



170 **Table 2. Models included in this study.**

Model	Dynamic vegetation	Vegetation representation	Key reference
CABLE-POP	No	Cohort	Haverd et al. (2018)
JULES	Yes	Average-individual	Clark et al. (2011)
LPJ-GUESS	Yes	Cohort	Smith et al. (2014)
LPJmL3.5	Yes	Average-individual	Sitch et al. (2003), Bondeau et al. (2007)
ORCHIDEE	Yes	Average-individual	Krinner et al. (2005)
SEIB-DGVM	Yes	Individual	Sato et al. (2007)



Table 3. Individual mortality processes included in the terrestrial biosphere models (TBMs) in this ensemble.

Conceptual grouping	Process	Example formulation (for actual model formulations see references in Table 1)	Included in model?					
			CABLE-POP	JULES	LPJ-GUESS	LPJmL	ORCHID-EE	SEIB-DGVM
Vitality	Growth efficiency	$mort_{greff} = \frac{k1}{1 + k2(\Delta C/LA)}$ where $k1$ and $k2$ are coefficients, ΔC is the annual biomass increment and LA is leaf area. $mort_{greff}$ is a fractional scalar, where 1 = 100% mortality.	X		X	X	X	X
	Self-thinning	if $\sum_{PFT} A_{PFT} > A_{max}$, then mortality occurs to reduce A_{PFT} , where A_{PFT} is the ground area covered by a particular PFT and A_{max} is the maximum allowable area coverage for all PFTs in a grid-cell.	X	X	X	X	X	
Disturbance	Disturbance	Random likelihood of stand destruction in any given year with a globally defined typical return time (e.g. 100 years)	X		X			X
	Fire	Thonicke et al. (2001) process-based fire model			X	X	X	X
Background	Max age/size	Trunk width exceeds maximum value, or increasing with age.			X			X
	Fixed turnover	Fixed turnover time for wood biomass (applicable in models using average individuals only)		X			X	
Heat	Heat	$mort_{heat} = \max \left[1, \frac{\sum_d \max (T_d - T_{mort}, 0)}{M_{full}} \right]$ where T_d is daily mean temperature, T_{mort} is a base temperature for mortality, and M_{full} is a temperature sum for 100% mortality. $mort_{heat}$ is a fractional scalar, where 1 = 100% mortality.				X ^a	X ^a	^b
Other	Bioclimatic limits	Multi-annual means of temperature fall outside a PFT specific range.			X	X	X	X
	Negative biomass	Biomass in any vegetation compartment becomes negative (NPP is more negative than living biomass)			X	X		

^a Only implemented for the boreal PFTs.

^b The original formulation of SEIB-DGVM includes heat stress mortality, but this function is now commonly turned off, as it was in this study.



Table 4. 1985-2014 global closed-canopy forest totals based on the CRU-NCEP-forced simulations and satellite-based methods.

Model	NPP (Pg C a⁻¹)	C_{veg} (Pg C)	τ_{NPP} (years)	τ_{turn} (years)	τ_{mort} (years)	τ_{fineroot} (years)
CABLE-POP	18.4	414.0	22.6	23.5	49.9	0.6
JULES	24.0	284.1	11.9	12.2	15.1	5.0
LPJ-GUESS	23.0	288.7	12.5	13.2	36.0	1.4
LPJmL	22.9	429.2	18.8	19.8	47.5	1.8
ORCHIDEE	31.8	432.0	13.6	14.2	26.1	1.7
SEIB-DGVM	29.9	421.0	14.1	14.7	30.1	1.7
Satellite-based	23.3 ^a	449.7 ^b	19.3 ^b	N/A	N/A	N/A

^a NPP calculated over 2000-2012.

^b Nominal base year in range 2000-2010.

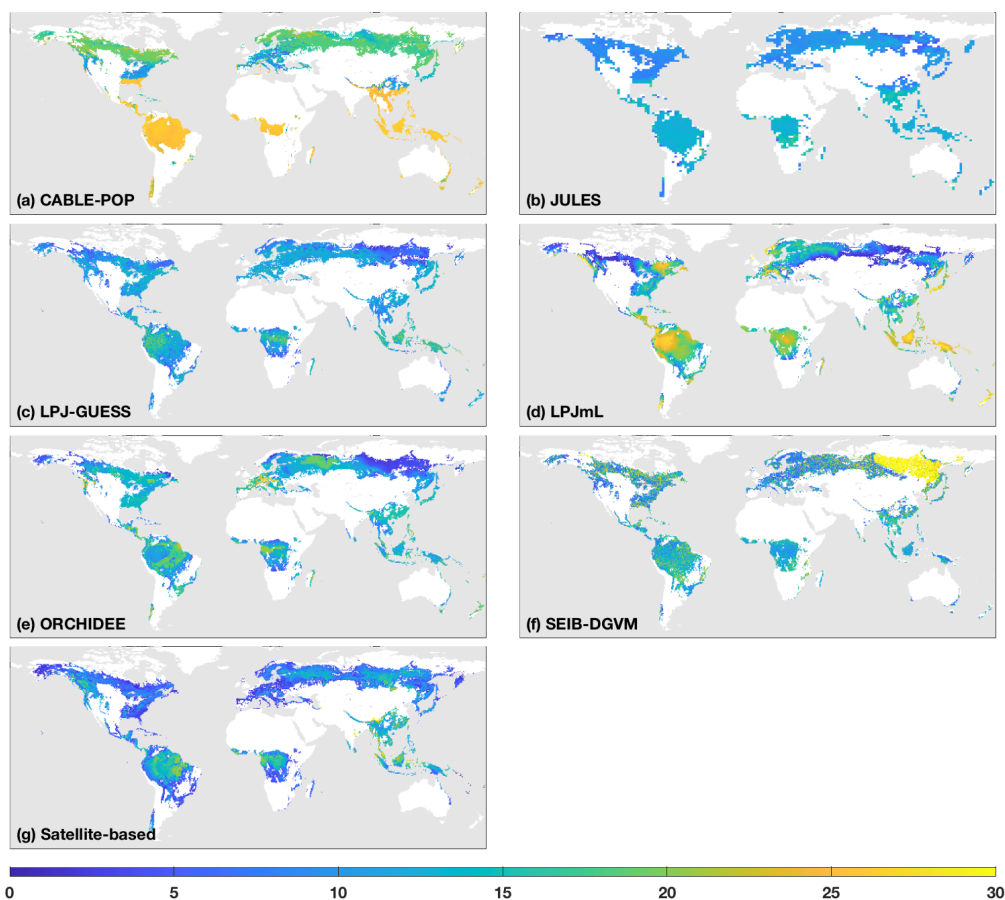


180

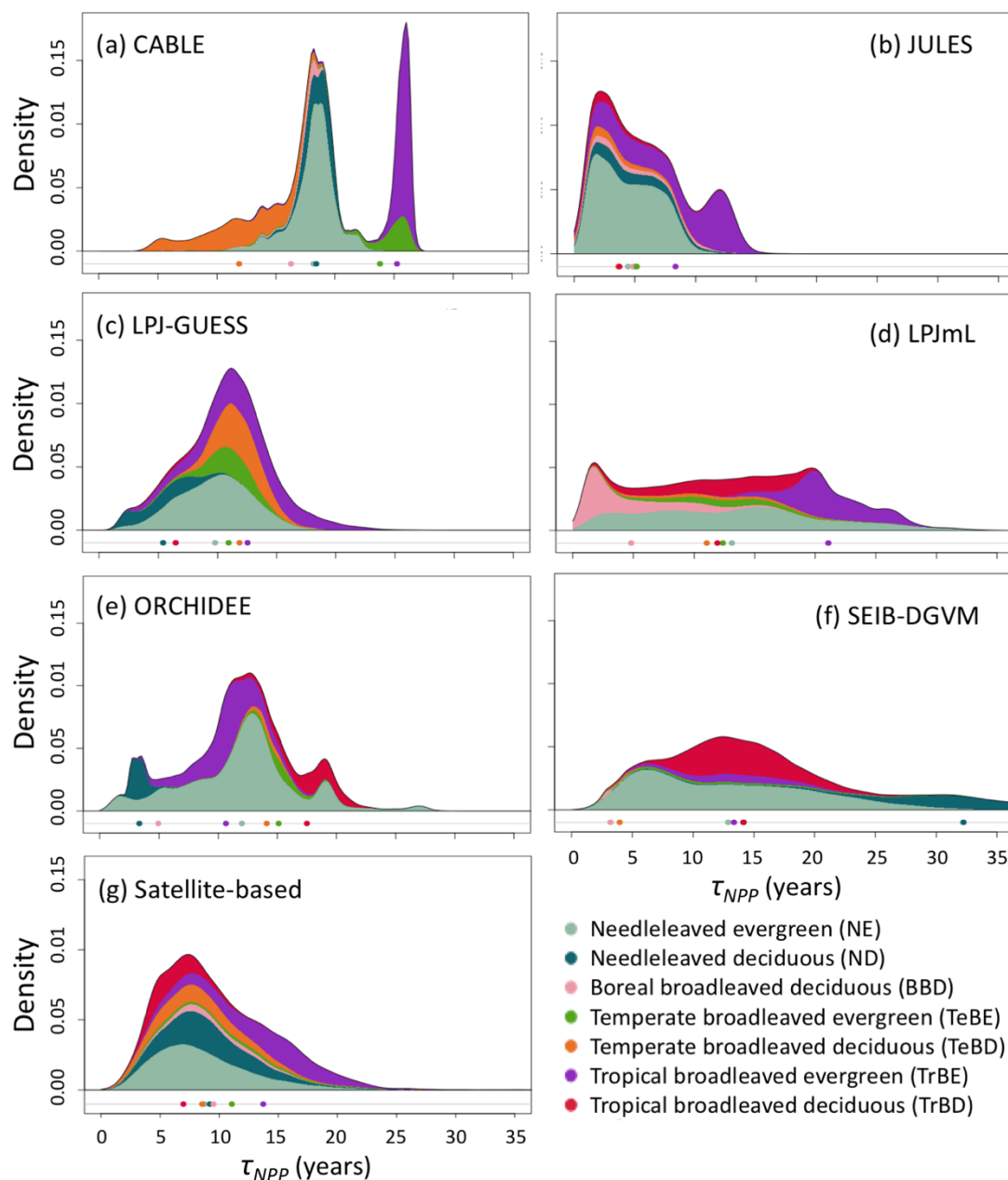
Table 5. Hypotheses resulting from the terrestrial biosphere models (TBMs) for controls on spatial and temporal variation in turnover time.

	Hypothesis	Mechanisms	Models exhibiting response
Existing situation (baseline)			
H1a	Investment in soft tissues is a relatively small fraction of NPP, implying relatively rapid turnover times for wood (τ_{mort}).	N/A	JULES
H1b	Investment in soft tissues is a relatively large fraction of NPP, implying relatively long turnover times for wood (τ_{mort}).	N/A	CABLE-POP, LPJ-GUESS, LPJmL, ORCHIDEE, SEIB-DGVM
H2	Variation in phenological turnover fluxes is as important as variation in mortality turnover fluxes, in driving spatial variation in τ .	N/A	CABLE-POP, LPJ-GUESS, LPJmL, ORCHIDEE
H3a	Carbon turnover times in tropical evergreen forests are much longer than for other forests, driven by long turnover times for wood.	N/A	CABLE-POP, LPJmL
H3b	Carbon turnover times in tropical evergreen forests are much longer than for other forests, driven by greater relative allocation of NPP to wood.	N/A	CABLE-POP, JULES, LPJ-GUESS, ORCHIDEE, SEIB-DGVM
H4a	The main driver of mortality carbon turnover fluxes in global forests is physical disturbance.	N/A	CABLE-POP, LPJ-GUESS
H4b	The main driver of mortality carbon turnover fluxes in global forests is low vitality.	N/A	JULES, LPJmL, SEIB-DGVM
Under environmental change			
H5	Shifts in relative PFT establishment rates and thus forest functional composition, rather than changes in the turnover rate of individual PFTs, dominate the response of τ to environmental change.	MP_{MR} , $M2c$, MP_{ST} vs. MI_{MR} , MI_{RA} , MI_{ST}	LPJmL, LPJ-GUESS ¹
H6	Establishment-driven shifts in functional composition and τ occur without large changes in mortality rates of established trees.	MP_{MR} , MP_{RA} , MP_{ST}	LPJ-GUESS ¹
H7a	Elevated atmospheric CO ₂ concentrations result in greater rates of mortality due to vitality-based processes because of increased competition for space as a result of increased NPP.	MI_{MR}	CABLE-POP, JULES, LPJ-GUESS, SEIB-DGVM ¹
H7b	Elevated atmospheric CO ₂ concentrations result in reduced rates of mortality because vitality-based processes are triggered less with increased NPP.	MI_{MR}	LPJmL, CABLE-POP ¹
H8a	Increased forest productivity results in much higher relative allocation to wood than soft tissue, partially compensating for, or even outweighing, reductions in τ_{mort} .	$MI_{\text{NPP,FS}}$	JULES, LPJ-GUESS, LPJmL, SEIB-DGVM
H8b	Increased forest productivity has very little effect on relative allocation between wood and soft tissues.	$MI_{\text{NPP,F}}$	CABLE-POP, ORCHIDEE

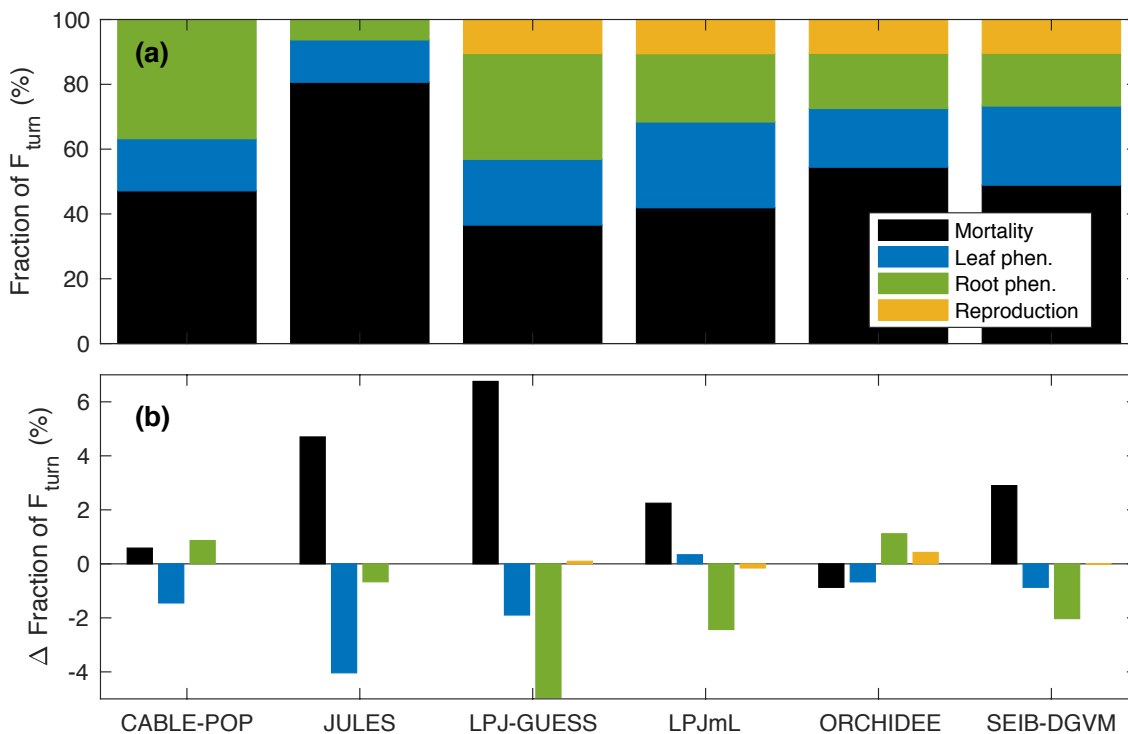
¹This hypothesis may hold in other TBMs here, although not positively identified in this study.



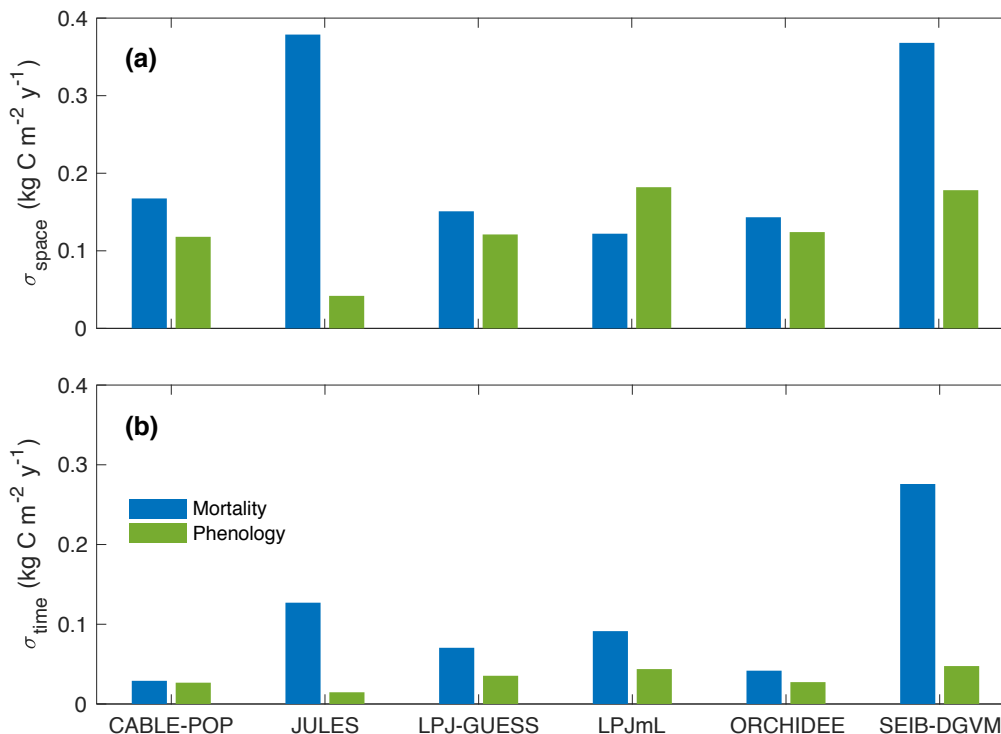
185 **Figure 1.** τ_{NPP} mean for the period 1985-2014 as forced by the CRU-NCEP climate (units of years). Colour scale is capped at 30 years. Maps show areas which are simulated as forest for each model and have at least 10% of the grid-cell covered by closed-canopy forest based on Hansen et al. (2013) (see Methods).



190 Figure 2. Density kernels for τ_{NPP} for the period 1985–2014 under CRU–NCEP climate calculated by forest type (see Methods) and
 superimposed to produce a global density kernel. Density is defined as fraction of total grid-cell number, including all grid-cells with
 at least 10% forest cover (i.e. masking as for Fig. 1). Circles underneath kernels show the mean turnover time for each forest type
 195 after weighing by the forest cover fraction of the grid cell and excluding grid cells with less than 10% forest cover (see Table S1 for
 forest type definitions). For the satellite-based kernels the observationally based forest types (Table S3) were used, with broadleaved-
 needleleaved mixed forest (MX) assigned to BBD and excluding other tropical forest (OTr) and other forest (Other) because no
 equivalent categories were reported for the models.



200 **Figure 3.** Fraction of global F_{turn} resulting from individual model processes. (a) For 1985-2014 in the CRU-NCEP-forced simulation. (b) Change in fraction of F_{turn} (percentage points) between 1985-2014 and 2070-2099 in the simulations forced by IPSL-CM5A-LR RCP 8.5 bias-corrected climate data. Black is mortality, light blue is leaf phenological turnover, green is root phenological turnover, and yellow is reproductive turnover.



205

210

Figure 4. Standard deviation of turnover fluxes for mortality (F_{mort}) and phenology (F_{phen}) across all grid-cells with at least 10% forest cover. (a) Standard deviation in space after first taking mean values over the period 1985-2014 from the CRU-NCEP-forced simulation. (b) Standard deviation in time, calculated by taking the variance on a 31-year running mean of turnover fluxes over the period 1985-2099 for each grid-cell in the simulations forced by IPSL-CM5A-LR RCP 8.5 bias-corrected climate data, and then taking the square root of the mean variance across all grid-cells. Spatial variation may be overestimated in SEIB-DGVM because of the large stochastic component to mortality that is not damped by multiple replications at the grid-cell level. Comparisons of absolute numbers from JULES with those of the other TBMs should be avoided because of the different spatial resolution used for JULES herein.

215

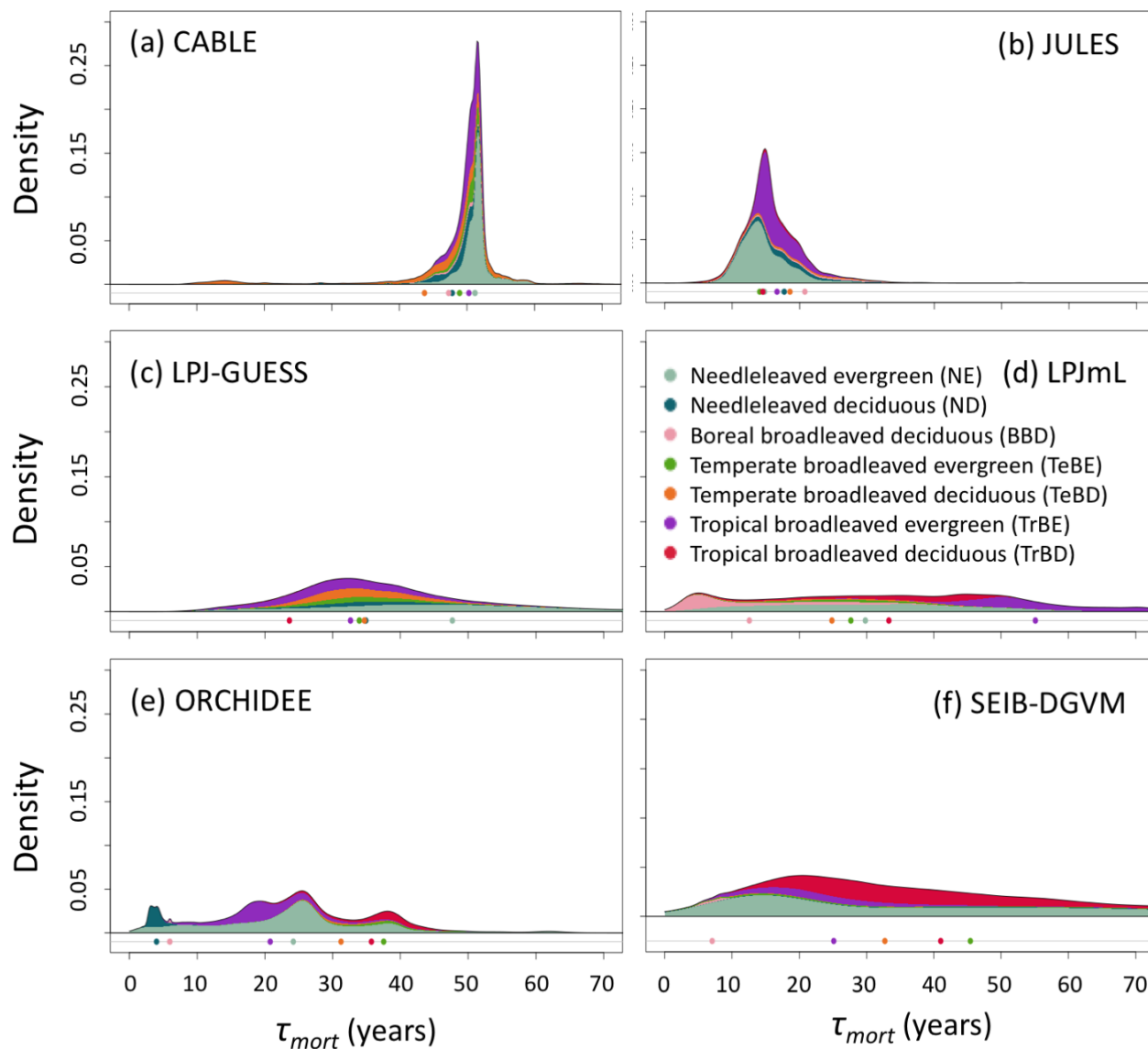
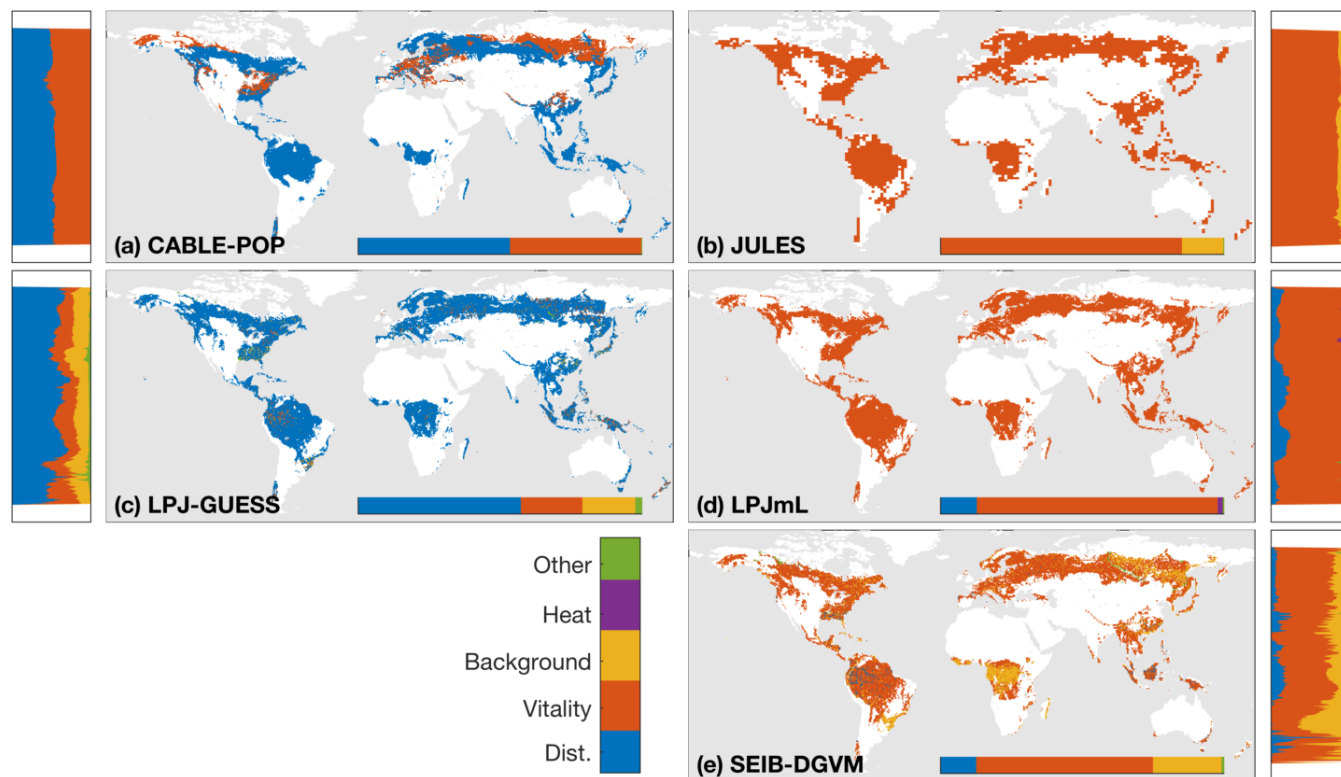
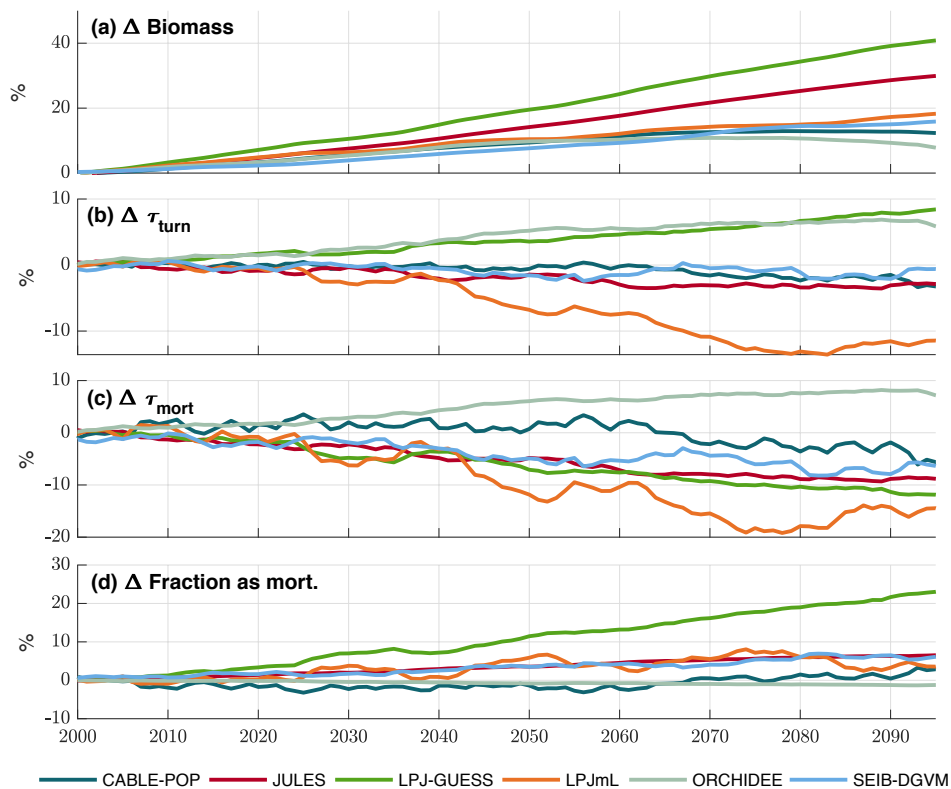


Figure 5. As for Fig. 2, but for turnover times due to mortality alone, τ_{mort} (C_{veg}/F_{mort}). Circles underneath kernels show the mean turnover time for each forest type.



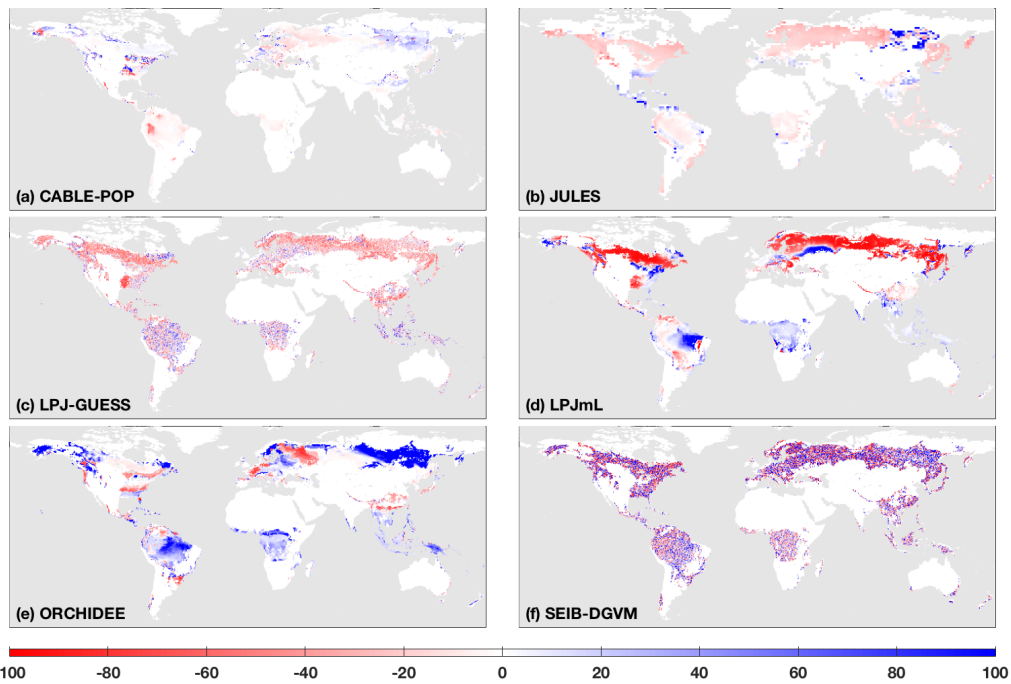
225

Figure 6. Dominant mortality process by carbon flux for the period 1985-2014 as forced by the CRU-NCEP climate. Bar insets indicate the fraction of the global mortality-driven turnover flux due to each mechanism, whilst vertical axes show the fraction due to each mortality process across latitude bands. Processes are grouped conceptually and equations and parameters used generally differ between models, as outlined in Table 2. "Dist." is mortality due to forest disturbance and may or may not conceptually include fire, depending on whether the model has an explicit fire mechanism. Vitality groups processes such as growth efficiency, self-thinning and more general competition. "Other" includes all processes that did not conceptually fit into one of the categories (Table 2). A breakdown of processes was not available for ORCHIDEE.



230

Figure 7. Simulated evolution of carbon residence times in the TBM simulations forced by IPSL-CM5A-LR RCP 8.5 bias-corrected climate data. (a) C_{veg} . (b) τ_{turn} ($C_{\text{veg}}/F_{\text{turn}}$). (c) τ_{mort} ($C_{\text{veg}}/F_{\text{mort}}$). (d) Fraction of total turnover due to mortality. Results are shown as an 11-year running mean.



235

Figure 8. Percentage change in τ_{mort} ($C_{\text{veg}}/F_{\text{mort}}$) mean between the periods 1985-2014 and 2070-2099 as forced by the IPSL-CM5A-LR climate (units of years). Masking as for Fig. 1.